THE UNIVERSITY OF MICHIGAN
COLLEGE OF ENGINEERING
Department of Chemical and Metallurgical Engineering

Final Report

DESIGN OF CHEMICAL REACTORS

Francis M. Donahue
Principal Investigator

Frederick L. Shippey
Dennis E. Stover
Leslie K. Anderson
Cary W. Halsted

ORA Project 33864

under contract with:

MEAD CORPORATION
CENTRAL RESEARCH LABORATORIES
CHILLICOTHE, OHIO

administered through:

OFFICE OF RESEARCH ADMINISTRATION ANN ARBOR

April 1970

enqm

UMR0918

TABLE OF CONTENTS

		Page
LIST OF ILLUSTRATIONS		
1.	SUMMARY	1
2.	INTRODUCTION	2
3.	DESIGN EQUATIONS FOR ELECTROLYTIC CELLS	3
	A. Voltage Balances	3
	B. Material Balances and Kinetics	5
4.	DESIGN EQUATIONS FOR MIXED POTENTIAL ELECTROLYSIS	10
5.	EXPERIMENTAL PROCEDURES AND EQUIPMENT	14
	A. Solution Preparation	14
	B. Experimental Procedures	14
	1. Open circuit potential measurements	14
	2. Kinetic measurements	14
	C. Equipment	15
	1. Test Cells	15
	2. Test Electrodes	15
6.	ANALYTICAL TECHNIQUES FOR POLYSULFIDE SULFUR	17
7.	ANODIC BEHAVIOR OF SULFIDE ION ELECTRODES	19
	A. Determination of Reaction Orders	19
	B. Activation Energy	21
	C. Standard Specific Rate Constant	22
	D. Polarization Behavior	22
	E. Further Comments on Complex Kinetics	22
8.	ANODIC AND CATHODIC BEHAVIOR OF OXYGEN ELECTRODES	35
9.	HYDROGEN EVOLUTION ON CARBON STEEL ELECTRODES	37
10.	CONCLUSIONS AND RECOMMENDATIONS	38
11.	REFERENCES	41

LIST OF ILLUSTRATIONS

Table — Page

I. Experimental Values of Activation Energy for the Oxidation of Sulfide Ion — 21

Figure

1. Schematic behavior of half-cell reactions. — 9

2. Schematic terminal voltage-current behavior. — 9

3. Three-phase mixed potential electrolysis scheme. — 13

4. Embodiment of a three-phase mixed potential electrolysis system with a provision for a driven mixed potential process. — 13

5. Photograph of the test electrode holder. — 16

6. Drawing of the tubing shaft used in the experiments using air as a reactant. — 16

7. Calibration curves for the spectrophotometric determination of polysulfide sulfur. — 18

8. Calibration curves for polysulfide sulfur using electrode potential measurements. — 18

9. Determination of the reaction order data for the oxidation of sulfide ion on platinum. — 24

10. Determination of the reaction order for the oxidation of sulfide ion on carbon electrodes. — 24

11. Determination of the reaction order with respect to hydroxyl ion for the oxidation of sulfide ion on carbon electrodes. — 25

12. Determination of the activation energy for the oxidation of sulfide ion on carbon electrodes. — 25

13. Polarization behavior of platinum electrodes for the oxidation of sulfide ion. — 26

LIST OF ILLUSTRATIONS (Concluded)

Figure		Page
14.	Polarization behavior of carbon electrodes for the oxidation of sulfide ion.	27
15.	Anodic and cathodic polarization behavior of Union Carbide electrodes for the air-alkali system at 35°C.	36
16.	Demonstration of the utility of "fundamental" half-cell studies to the phenomena of fuel cell, driven fuel cell, and mixed potential electrolysis systems.	40

1. SUMMARY

The theoretical aspects of the project were completed including the design equations for mixed potential electrolysis (not contained in the original proposal). The resulting equations indicated that laboratory experiments of a fundamental nature are essential to a priori design and optimization of electrochemical reactors.

The fundamental experiments on the electrochemical properties of sulfide, sulfur, oxygen reduction and evolution, and hydrogen evolution were substantially completed during the contract period. However, a complete characterization of the electrode processes, e.g., determination of reaction mechanism, was not attempted.

An analytical method for measuring polysulfide streams was found based upon the measured potential difference between a reference electrode (saturated calomel electrode, S.C.E.) and a sulfur-sulfide "sensitive" electrode. A sulfide ion electrode (Orion Model 94-16) was found to give a good correlation line, $(d\varphi/d\log S_{-2})_{\text{total S = const}} = 0.090$ volt, which is reasonably sensitive to changes anticipated in the electrolytic cell. However, it was decided that a platinum wire electrode (much less bulk), which had a correlation line with a higher slope compared to the sulfide ion electrode, would be used in the prototype electrolytic cell.

The final phase of the proposed research, viz., testing of the theoretical design equations in a lab-scale reactor, is incomplete. Consistent with the principles underlying the theoretical basis of the current work, it was virtually impossible to size the reactor volume, pump flow rates, etc., prior to the analysis of the half-cell reaction studies—particularly the sulfide-sulfur system. Consequently, the purchase orders for the equipment were placed during the summer and early fall of 1969. At the present time no useful data have been taken with the prototype reactor due to "normal" start-up problems.

2. INTRODUCTION

There is a virtual absence of a rational, formalistic design philosophy for electrochemical reactors. It was the intent of the principal investigator and his co-workers to fill this void by theoretical and experimental work on systems of interest to the sponsor, viz., sulfide ion oxidation in an electrolysis cell or in some sort of "fuel cell" configuration. Within the context of the nature of laboratory work and the flexibility of the principal investigator (see below) the project has been successful, albeit incomplete.

The theoretical design equations for electrochemical reactors (electrolytic cells and/or batteries or fuel cells) are derived herein on the basis of electrochemical thermodynamics and kinetics and chemical reactor design theory. This satisfies Phase I of the contract between the University and Mead Corporation (dated November 27, 1968).

However, the principal investigator, as a consequence of his consulting activities with the Mead Corporation, perceived an additional requirement from this project which had not been contracted for, viz., an analysis of the design criteria for mixed potential electrolytic cells. Further, it was evident that an instantaneous, reliable method for analyzing reactor effluent streams containing polysulfide sulfur (when the total sulfur content of the stream was known) would be needed in the event the sponsor should commercialize the process. Both of these tasks were included in the project and reported herein with the tacit approval of the technical liaison personnel at the Mead Corporation Research Laboratories.

Phase II of the contract involved bench-scale kinetic studies of various combinations of electrode materials and electrolytic solutions. Although the overall scope of these studies was neither exhaustive nor deep, the experiments were relevant to the studies at hand and within the "time frame" permitted by the contract period. The results are discussed in the bulk of the report.

Phase III, viz., the design, construction, and operation of small prototype reactors, is incomplete. While the design and construction are complete, no meaningful data have been obtained at this time due to the "bugs" normally encountered on start-up.

3. DESIGN EQUATIONS FOR ELECTROLYTIC CELLS

A. VOLTAGE BALANCES

All electrochemical cells (both energy consuming, i.e., electrolysis cells, and energy generating, i.e., batteries and fuel cells) operate in the same fashion. The open circuit terminal voltage (in the absence of a flow of current in the cell) is given by

$$-\frac{\Delta G}{n\mathcal{F}} = \varepsilon_o \qquad (3\text{-}1)$$

where ΔG is the Gibbs Function change for the overall cell reaction (g-calories/g mole of a "basis" species), n is the stoichiometric coefficient of electrons with respect to the "basis" species (g-equivalents/g mole of "basis" species), $\mathcal{F}$ is the Faraday constant (23,060 g-calories-volt^{-1} - g-equivalent^{-1}), and ε_o is the open circuit terminal voltage (volt). Based upon the concept of spontaneity of chemical reactions, equation 3-1 shows that batteries (energy generating cells) have positive open circuit terminal voltages while electrolysis cells have negative terminal voltages.

The open circuit terminal voltage of an electrochemical cell, in terms of the electrode potentials of the half-cell reactions, is

$$\varepsilon_o = \varphi_{oc} - \varphi_{oa} \qquad (3\text{-}2)$$

where φ_{oc} is the reversible potential* of the cathodic half-cell reaction and φ_{oa} is the reversible potential* of the anodic half-cell reaction. A voltage balance on an electrochemical cell through which a current flows yields

$$\varepsilon_I = \varphi_{Ic} - \varphi_{Ia} - I\,R_{int} \qquad (3\text{-}3)$$

where ε_I is the terminal voltage observed for a current load (I), φ_{Ic} is the electrode potential of the cathodic half-cell reaction under load, φ_{Ia} is that for the anodic half-cell reaction and R_{int} is the internal resistance of the

*The sign used in this analysis agree with the I.U.P.A.C. convention, viz., the sign of the base metals (e.g., iron, zinc, etc.) are negative when referenced to a standard hydrogen electrode.

cell (including electrolyte resistance and that of the separator). From electrochemical kinetics, overvoltage is defined as

$$\eta = \varphi_I - \varphi_o \tag{3-4}$$

Substitution of equation (3-4) in (3-3)

$$\varepsilon_I = \varphi_{oc} + \eta_c - \varphi_{oa} - \eta_a - I R_{int} \tag{3-5}$$

From the definition of overvoltage one notes that the overvoltage for the cathodic half-cell reaction, η_c, is inherently negative. Substitution of equation (3-2) in (3-5)

$$\varepsilon_I = \varepsilon_o + \eta_c - \eta_a - I R_{int} \tag{3-6}$$

Equation (3-6) shows that the terminal voltage under load is <u>always</u> less (i.e., more negative) than the open circuit terminal voltage. Equation (3-6) indicates that the terminal voltage of an electrochemical cell may be deduced from a knowledge of the polarization behavior of the respective half-cell reactions and the internal resistance of the cell. Unfortunately, equation (3-6) does not express certain design considerations explicitly, e.g., electrode area, electrolyte flow rate, etc. Consequently, equation (3-6) can be used only as a starting point for an analysis of the design criteria for electrochemical reactors.

Figure 1 is a graphical representation of the polarization behavior of the separated anodic and cathodic half-cell reactions for batteries (Figure 1a) and electrolytic cells (Figure 1b). It is observed that, although, for example, the relative locations of the anodic polarization curves in the two sketches are different, the shapes of the respective polarization curves are similar. From studies of the individual half-cell reactions (normal polarization experiments) one can construct pairs of oxidation-reduction reactions which could represent batteries or electrolysis cells depending upon the sign of the open circuit terminal voltage.

If one constructs curves similar to Figure 1 and then determines the theoretical terminal voltage as a function of the current "passing" through the cell, a terminal voltage-current diagram may be plotted (see the solid curves in Figure 2). In order to determine the "true" voltage-current curve, one would have to evaluate the internal resistance and subtract the voltage drop due to the "internals" (see the dashed curves in Figure 2).

B. MATERIAL BALANCES AND KINETICS

Levenspiel[1] has outlined the steps necessary to determine the design equations for chemical reactors. It is convenient to use these design equations for electrochemical reactors provided one realizes that there are actually <u>two</u> reactors, viz., the cathode and the anode, which are coupled by the total current passing through the cell.

Consider the following overall cell reaction

$$\nu_B B + \nu_c C \rightarrow \nu_D D + \nu_F F \tag{3-7}$$

If one uses species B as the "basis" material (the choice is arbitrary; however, it is frequently prudent to focus on the "limiting" reactant, the concentration of any species, e.g., J, at any time is

$$[J] = [B]_o\left(\frac{[J]_o}{[B]_o} + \frac{\nu_J}{|\nu_B|} X\right) \tag{3-8}$$

where the brackets denote the concentrations of the respective species, the zero subscripts denote the feed concentrations and X is the conversion, i.e.,

$$X = \frac{\text{moles of species B reacted}}{\text{moles of species B fed}} \tag{3-9}$$

It will be assumed that the anodic half-cell reaction is

$$\nu_B B \rightarrow \nu_D D + \nu_e e^- \tag{3-10}$$

According to Donahue[2] the Tafel form of the Butler equation may be written as

$$i_p = \frac{\nu_e}{\nu_B} k_a^o [B]^\gamma \exp\left[\frac{\varphi_{ia} - \varphi_a^o}{\beta_a}\right] \tag{3-11}$$

where i_p is the net anodic current density (amp cm^{-2}), $\mathcal{F}$ is the Faraday constant (96,500 coulombs g-equivalent^{-1}), k_a^o is the specific rate constant of the anodic half-cell reaction at the <u>standard electrode potential</u>, γ is the chemical reaction order with respect to species B, φ_i is the electrode potential of the anodic partial process (half-cell reaction) at a current density of i_p, φ^o is the standard

electrode potential and β_a is a Tafel constant. Further, the rate of an electrochemical reaction based upon species B may be written

$$-r_B = \frac{i_p}{\left|\frac{\nu_e}{\nu_B}\right| \mathcal{F}} \tag{3-12}$$

If one assumes that the electrochemical reactor under consideration behaves like a continuous stirred tank reactor (CSTR)*, a steady-state material balance on the anodic partial process gives

$$-r_B A_a = F_{Bo} X \tag{3-13}$$

where A_a is the area of the anode and F_{Bo} is the mole feed rate of species B (g-moles of B sec^{-1}). The space time (sec) τ_a, for the anodic partial process is

$$\tau_a = \frac{V_a}{v_{oa}} = \frac{F_{Bo} V_a X}{v_{oa} (-r_B) A_a} \tag{3-14}$$

where V_a is the volume of the anolyte (cm^3) and v_{oa} is the volumetric feed rate of anolyte (cm^3 sec^{-1}). Substitution of equations (3-8) and (3-12) in (3-11) and (3-14)

$$\tau_a = \left(\frac{F_{Bo}}{v_{oa}}\right)^{1-\gamma} \frac{V_a X}{k_a^o A_a (1-X)^\gamma} \exp\left[-\frac{\varphi_{ia}-\varphi_a^o}{\beta_a}\right] \tag{3-15}$$

Rearranging and taking logs

$$\varphi_{ia} = \varphi_a^o + b_a \log\left\{\left(\frac{F_{Bo}}{v_{oa}}\right)^{1-\gamma} \frac{V_a X}{k_a^o \tau_a A_a (1-X)^\gamma}\right\} \tag{3-16}$$

---

*Levenspiel[1] also discusses batch and plug flow reactors, but for simplicity only CSTR's will be treated here.

where b_a is the anodic Tafel slope ($2.3\beta_a = b_a$).

The cathodic partial process is assumed to be

$$\nu_c C + \nu_e e^- \rightarrow \nu_F F \tag{3-17}$$

If the cathode is assumed to behave like a CSTR, the steady-state material balance is

$$-r_c A_c = F_{Bo} \frac{\nu_c}{\nu_B} X \tag{3-18}$$

The Tafel form of the Butler equation is

$$i_p = \frac{\nu_e}{\nu_c} \mathcal{F} k_c^o [C]^\delta \exp\left[-\frac{(\varphi_{ic} - \varphi_c^o)}{\beta_c}\right] \tag{3-19}$$

The space time for the cathode reaction is

$$\tau_c = \frac{V_c}{v_{oc}} = \frac{\nu_c F_{Bo} V_c X}{\nu_B (-r_c) v_{oc} A_c} \tag{3-20}$$

Substitution of equations (3-8) and (3-12)* in (3-19) and (3-20)

$$\tau_c = \frac{\nu_c (F_{Bo})^{1-\delta} (v_{oa})^\delta V_c X}{\nu_B k_c^o A_c v_{oc} \left(\frac{F_{co}}{F_{Bo}} - \frac{\nu_c}{\nu_B} X\right)^\delta} \exp\left[\frac{\varphi_{ic} - \varphi_c^o}{\beta_c}\right] \tag{3-21}$$

Rearranging and taking logs

$$\varphi_{ic} = \varphi_c^o - b_c \log\left\{\frac{\nu_c (F_{Bo})^{1-\delta} (v_{oa})^\delta X}{\nu_B k_c^o A_c \left(\frac{F_{co}}{F_{Bo}} - \frac{\nu_c}{\nu_B} X\right)^\delta}\right\} \tag{3-22}$$

*Based on the rate of reaction of species C.

Substitution of equations (3-16) and (3-22) in (3-3)

$$\varepsilon_I = \varphi_c^o - \varphi_a^o - b_c \log\left\{\frac{\nu_c (F_{Bo})^{1-\delta} (v_{oa})^{\delta} X}{\nu_B k_c^o A_c \left(\frac{F_{co}}{F_{Bo}} - \frac{\nu_c}{\nu_B} X\right)^{\delta}}\right\}$$

$$- b_a \log\left\{\left(\frac{F_{Bo}}{v_{oa}}\right)^{1-\gamma} \frac{V_a X}{k_a^o \tau_a A_a (1-X)^{\gamma}}\right\} - I R_{int} \qquad (3\text{-}23)$$

The total current is related to the conversion of species B by

$$I = \left|\frac{\nu_e}{\nu_B}\right| \mathfrak{F} F_{Bo} X \qquad (3\text{-}24)$$

Further, for equal area, parallel planar anodes and cathodes it may be shown that

$$R_{int} = \frac{1}{A^2} (\rho_a V_a + \rho_c V_c + R_s A) \qquad (3\text{-}25)$$

where ρ_a and P_c are the specific resistances (ohm cm) of the anolyte and catholyte, respectively, and R_s is the resistance of the separator (ohm-cm^2). Substitution of equations (3-24) and (3-25) in (3-23)

$$\varepsilon_I = \varepsilon^o - b_c \log\left\{\frac{\nu_o (F_{Bo})^{1-\delta} (\nu_{oa})^{\delta} X}{\nu_B k_c^o A_c \left(\frac{F_{co}}{F_{Bo}} - \frac{\nu_c}{|\nu_B|} X\right)^{\delta}}\right\}$$

$$- b_a \log\left\{\left(\frac{F_{Bo}}{v_{oa}}\right)^{1-\gamma} \frac{V_a X}{k_a^o \tau_a A_a (1-X)^{\gamma}}\right\}$$

$$- \left|\frac{\nu_e}{\nu_B}\right| \frac{\mathfrak{F} F_{Bo} X}{A^2} (\rho_a V_a + \rho_c V_c + R_s A) \qquad (3\text{-}26)$$

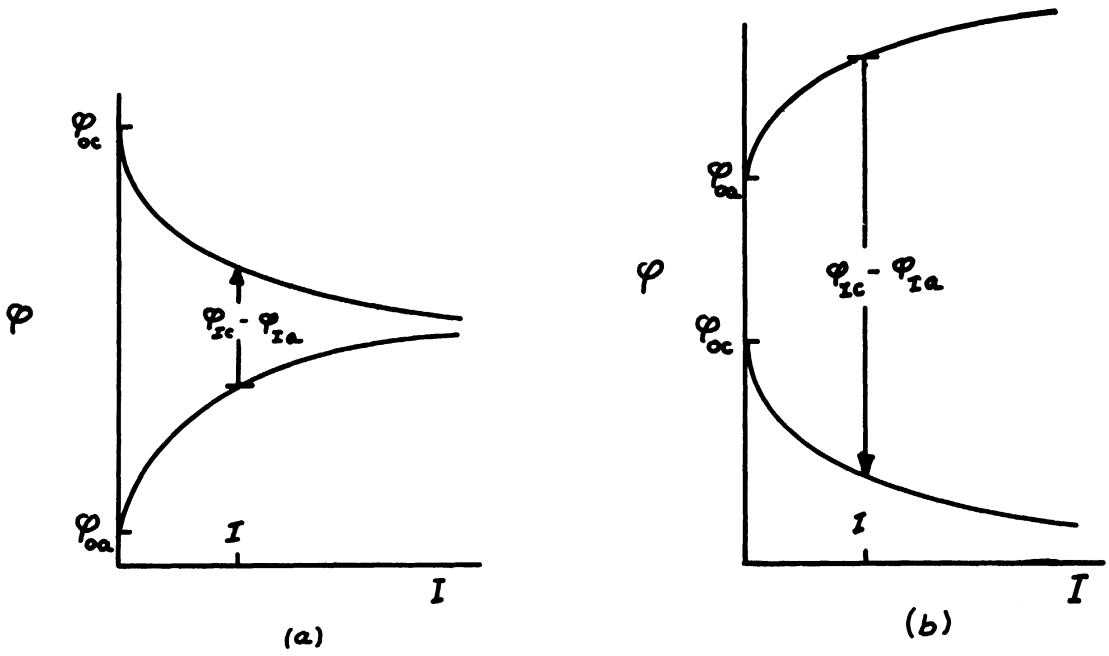

Figure 1. Schematic behavior of half-cell reactions for (a) batteries, and (b) electrolytic cells.

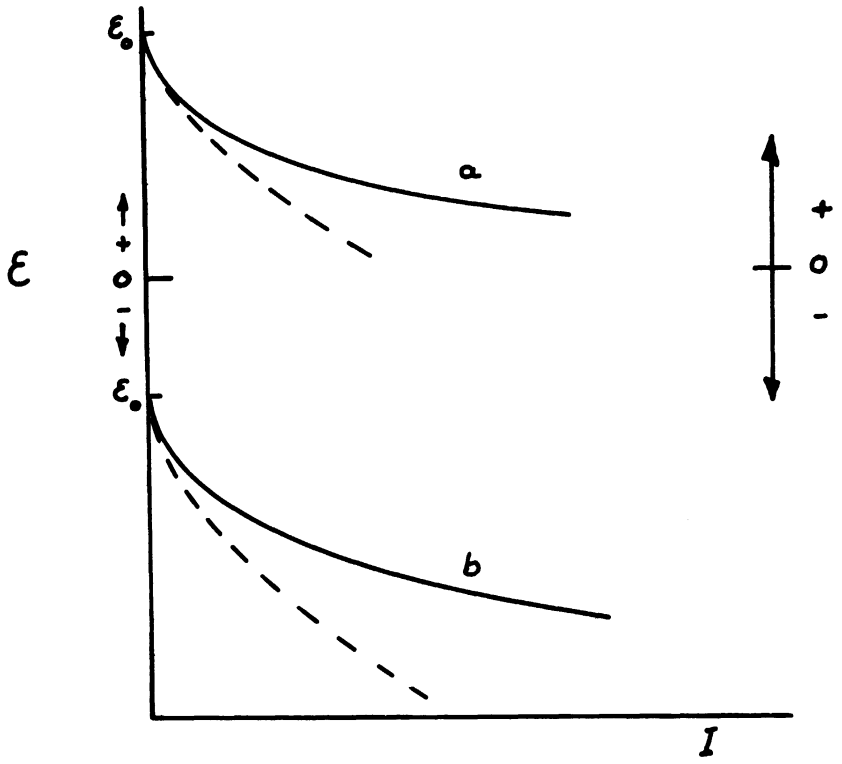

Figure 2. Schematic terminal voltage-current behavior for (a) batteries, and (b) electrolytic cells without IR (solid lines) and including IR (dashed lines).

4. DESIGN EQUATIONS FOR MIXED POTENTIAL ELECTROLYSIS

A significant development in the association between the Mead Corporation and The University of Michigan was the observation by Smith,[3] and the subsequent hypothesis by Donahue,[4] of the mixed potential nature of spontaneous and concomitant oxidation of a suitable oxidizable species and reduction of an appropriate oxidizing agent, e.g., oxygen, at a single electrode in the absence of an external source or sink for electrons. Initially, there was apprehension by the Mead Corporation that such a process (a) fell outside the realm of electrochemical processing and (b) if it were electrochemical, that it was irrelevant to the University project. Donahue[4] has amply explained that the process is electrochemical, and it remains to demonstrate the applicability of the foregoing analysis to the mixed potential electrolysis.

A mixed potential system is effectively an electrochemical generator which is short circuited, i.e., there is no potential difference between the cathodic and anodic partial processes. Both partial processes take place at the same electrode surface which, assuming a high surface electronic conductivity, is an equipotential surface. Analogous to the development of the normal electrolytic cell, a mixed potential system where reactants and products are soluble in the electrolytic phase yields (from equation (3-23))

$$0 = \varphi_c^o - \varphi_a^o - b_c \log \left\{ \frac{\nu_c (F_{Bo})^{1-\delta} (v_{oa})^{\delta} X}{\nu_B k_c^o A_c \left(\frac{F_{co}}{F_{Bo}} - \frac{\nu_c}{\nu_B} X \right)^{\delta}} \right\} - b_a \log \left\{ \left(\frac{F_{Bo}}{v_{oa}} \right)^{1-\gamma} \frac{v_{oa} X}{k_a^o A_a (1-X)^{\gamma}} \right\} \qquad (4\text{-}1)$$

Equation (4-1) may be rearranged

$$(b_a + b_c) \log \frac{F_{Bo} X}{A} + (\delta b_c + \gamma b_a) \log \left(\frac{v_{oa}}{F_{Bo}} \right) - b_c \log \left[\frac{\nu_B k_c^o \left(\frac{F_{co}}{F_{Bo}} - \frac{\nu_c}{\nu_B} X \right)^{\delta}}{\nu_c} \right]$$

$$-b_a \log \left[k_a^o (1-X)^\gamma \right] = \varepsilon^o \qquad (4\text{-}2)$$

Equation (4-2) describes the behavior of a mixed potential system in terms of process design variables and in terms of electrochemical parameters identical to those for the electrolysis cell.

Another mixed potential system which is of more immediate interest to the Mead Corporation is shown in Figure 3. This is the so-called "three-phase" system where an electrolytic phase containing the reactant for the anodic partial process is separated from the gaseous oxidant by an electronically conducting, electrolytically-wetted gas diffusion membrane (electrode). For simplicity, the overall reaction and the partial processes are assumed to be given by equations (3-7), (3-10), and (3-17), respectively. It is further assumed that the product of the cathodic partial process, F, is not gaseous and dissolves in the electrolyte.

Assuming that the electrolyte-electrode system behaves like a CSTR, the electrode potential of the anodic partial process is

$$\varphi_{ia} = \varphi_a^o + b_a \log \left[\left(\frac{F_{Bo}}{\nu_{oa}} \right)^{1-\gamma} \frac{X}{k_a^o A (1-X)^\gamma} \right] \qquad (4\text{-}3)$$

It is assumed that the pressure of oxidant gas, p_c, is kept constant, the cathodic electrode potential is

$$\varphi_{ic} = \varphi_c^o - b_c \log \left[\frac{\nu_c F_{Bo} X}{\nu_B k_c^o p_c^\epsilon A} \right] \qquad (4\text{-}4)$$

where ϵ is the reaction order for the oxidant gas. Equating equations (3-16) and (4-4), i.e., for the conditions of the mixed potential system, and collecting terms

$$\varepsilon^o = (b_a + b_c) \log \left[\frac{F_{Bo} X}{A} \right] - b_a \log \left[\left(\frac{F_{Bo}}{\nu_{oa}} \right)^\gamma \frac{\nu_{oa} k_a^o (1-X)^\gamma}{X} \right] - b_c \log \left[\frac{\nu_B k_c^o p_c^\epsilon}{\nu_c} \right] \qquad (4\text{-}5)$$

It should be noted that equations (4-2) and (4-5) do not offer as many "degrees of freedom" for process design variation as does the normal electrolytic cell. This is due to the fact that the mixed potential system has a unique value of the "terminal voltage," viz., zero, while the electrolytic cell has an infinite number of possiblities.

An increase in the rate of generation of both the anodic and cathodic products is feasible if a pair of mixed potential electrodes are connected to an external power supply. In this way one of the electrodes is polarized anodically (thereby, increasing the rate of generation of the anodic product) while the other is polarized cathodically. The voltage supplied to the mixed potential electrodes in such an arrangement is

$$\varepsilon_I = \varepsilon^\circ - (b_a + b_c) \log\left[\frac{F_{Bo} X}{A}\right] + b_c \log\left[\frac{\nu_B k_c^\circ p_c^\epsilon}{\nu_c}\right]$$

$$- I R_{int} + b_a \log\left[\left(\frac{F_{Bo}}{\nu_{oa}}\right)^\gamma \frac{\nu_{oa} k_a^\circ (1-X)^\gamma}{X}\right] \qquad (4\text{-}6)$$

The voltage necessary for such a "driven system" would be on the order of tenths of a volt for moderate increases of conversion rate, e.g., increasing the rate of reaction by a factor of ten (compared to the mixed potential rate would require a voltage equal to the sum of the Tafel slopes and the voltage drop due to the electrolyte resistance, i.e.,

$$\varepsilon_I \text{ (tenfold rate)} = b_a + b_c + I R_{int} \qquad (4\text{-}7)$$

Although a number of possible configurations have been proposed (e.g., discussions among Knowles, Smith, Sanders, and Donahue), an interestingly utilitarian and flexible system is shown schematically in Figure 4. A cross-section of a "shell and tube heat exchanger" reactor is used with the tube bundles fabricated from cylindrical gas diffusion electrodes (porous nickel, carbon, promoted carbon, etc.). The tube side of the reactor is fed reactant gas at constant pressure. The shell side of the reactor contains the flowing electrolyte and the other reactant species. An auxiliary power supply is shown which can be used to "drive" the mixed potential electrodes.

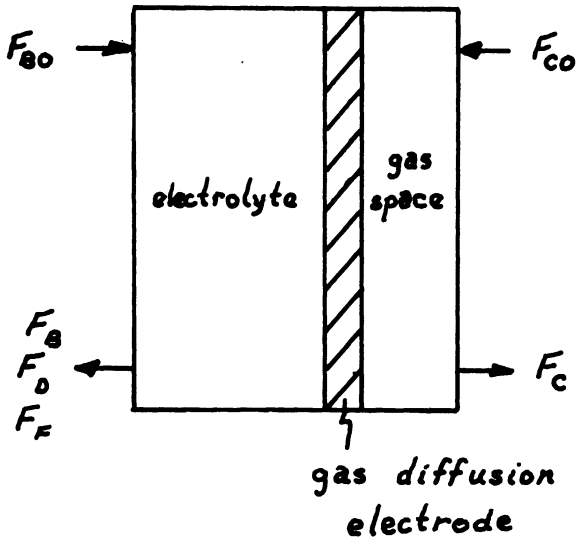

Figure 3. Three-phase mixed potential electrolysis scheme.

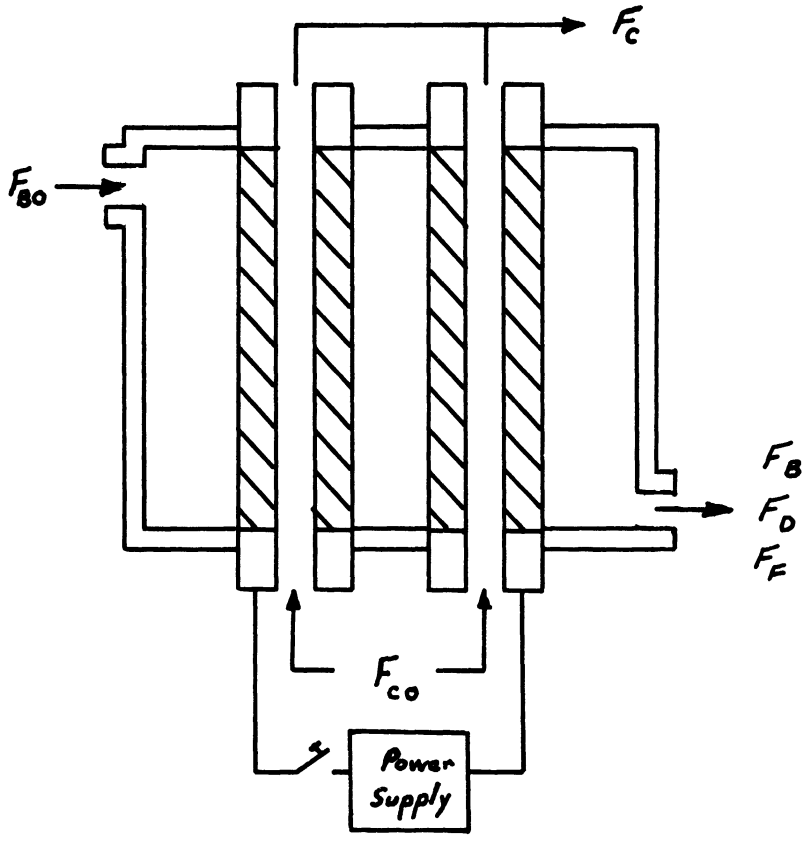

Figure 4. Embodiment of a three-phase mixed potential electrolysis system with a provision for a driven mixed potential process.

5. EXPERIMENTAL PROCEDURES AND EQUIPMENT

A. SOLUTION PREPARATION

A stock 1.0M NaOH solution was prepared by diluting 40.0 gm of Baker Reagent grade NaOH in 1 liter of doubly distilled water. This solution was then purged of oxygen by bubbling Matheson prepurified nitrogen through it for 16 hours.

Electrolytic solutions with a total sulfur concentration of 1.0M were prepared from Mallinckrodt reagent grade Na_2S $9H_2O$ and Mallinckrodt sublimed powder S. The ratio of S^{-2} to S was varied from one to four. The mixing was achieved by adding 1 liter of the NaOH stock solution to preweighed quantities of Na_2S and S. This solution was heated to effect dissolution, cooled to room temperature, and used immediately as the test electrolyte.

B. EXPERIMENTAL PROCEDURES

1. Open Circuit Potential Measurements

Experiments were performed to determine the effect of variations of the Na_2S and S concentrations in 1M NaOH solution on the open circuit potential of a sulfide ion electrode (orion Model 94-16) versus a S.C.E. Solutions prepared as described above were studied as soon as they cooled to room temperature (27°C). The potential was measured with a Digitec D.C. voltmeter (Model 201). Readings taken on standing at room temperature varied little with time.

2. Kinetic Measurements

The galvanostatic pulse technique (~10 sec pulse) was employed to obtain kinetic information. The pulses were alternatingly anodic and cathodic in an attempt to preserve the concentration integrity of the system. The temperature region from 35°C to 60°C was investigated. Various ratios of the Na_2S to S concentrations (total sulfur 1.0M) were investigated in 1.0M NaOH supporting electrolyte.

The test cell utilized the normal three electrode configuration with a platinized platinum electrode serving as the counter electrode. The reference electrode was a saturated Calomel electrode (Beckman No. 39402) with a luggin capillary extension to the surface region of the test electrode. Smooth platinum foil and Stackpole No. 139 porous carbon electrodes were studied as the test electrode (Area = 1.25 cm^2).

Preliminary kinetic studies were also performed in the 5.0M NaOH electrolyte (no sulfur present) with an air test electrode. Union Carbide type T2 and T3 electrodes were studied in a forced air system.

C. EQUIPMENT

1. Test Cells

The pyrex glass electrolytic cell is shown in Figure 5. The auxillary (A.E.) and reference (R.E.) electrodes are separated from the test electrode (T.E.) region by fritted glass disk to inhibit the transport of reaction products. The cell is sealable and experiments were performed in a nitrogen atmosphere. The working volume of the cell is 600 ml.

2. Test Electrodes

The nylon electrode holder for the platinum and carbon electrodes is also shown in Figure 5. The copper shaft was replaced with the tubing configuration shown in Figure 6 during the experiments with the air electrode.

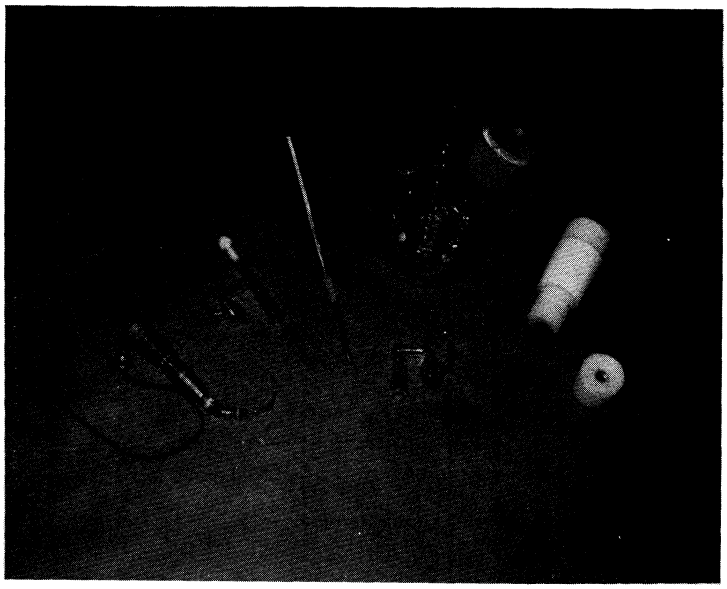

Figure 5. Photograph of the test electrode holder.

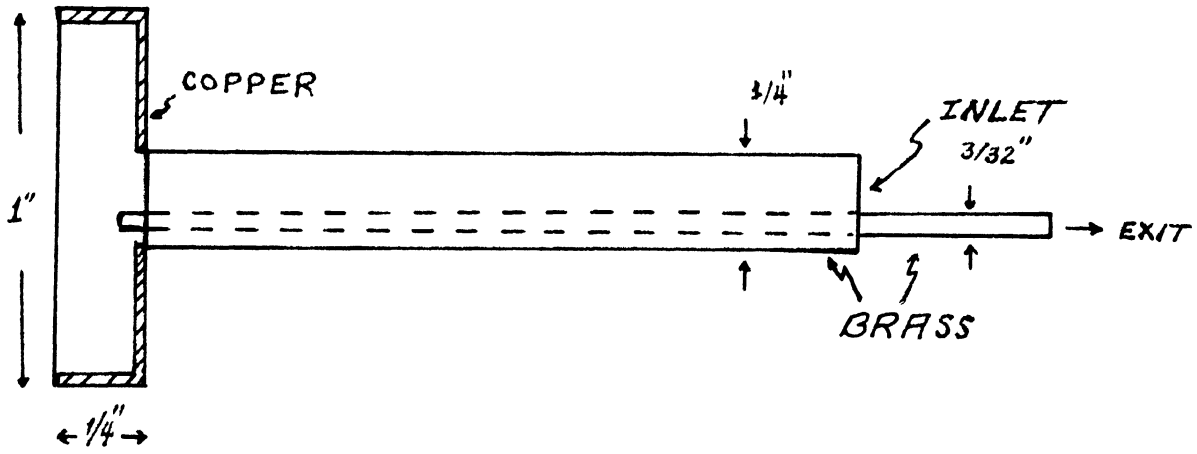

Figure 6. Drawing of the tubing shaft used in the experiments using air as a reactant.

6. ANALYTICAL TECHNIQUES FOR POLYSULFIDE SULFUR

In anticipation of the prototype reactor studies and/or the sponsor's commercialization of the polysulfide process, it was considered essential to develop an instantaneous, nondestructive quantitative analysis procedure for polysulfide sulfur. In principle such a technique could permit the analysis of transient reactor phenomena or the control of a commercial process.

Because of the dark color of the polysulfide solutions, it was assumed that spectrophotometric analyses would yield such a quantitative procedure. The spectra of a number of polysulfide solutions obtained with a Bausch and Lomb Model 600 Spectrophotometer showed a maximum absorption in the vicinity of 630 millimicrons. However, a plot of the percent transmittance (% T) vs. x-value revealed curves which did not yield single-valued x-values for an observed transmittance (Figure 7). Consequently, the optical approach to a solution was abandoned.

An Orion Model 94-16 specific sulfur ion electrode was obtained. In principle, a sulfide ion electrode should be relatively insensitive to changes in the sulfide ion activity, viz., a change of 30 mv per power of ten change in the activity. It was assumed, however, that the complexing of dissolved sulfur with the sulfide ion would decrease the sulfide ion activity to a greater extent than the nominal concentration would indicate. The slope of the measured sulfide ion electrode potential was three times the theoretical value for solutions containing polysulfide sulfur (see Figure 8a) in agreement with the hypothesis.

In the course of the kinetics experiments, it became evident that a platinum electrode was even superior to the specific ion electrode, yielding a slope which was approximately five times the theoretical slope (see Figure 8b). The data points were obtained using an electrometer and (because of the inability to read small changes on a large scale setting) are accurate to about $\pm$ 5 millivolts. In the latter stages of the work using carbon electrodes the precision of experiments was improved through the use of an API Digital Voltmeter. However, the intrinsic unreliability of the carbon electrodes (in terms of their utility as quantitative analysis electrodes) did not permit us to take advantage of the enhanced precision.

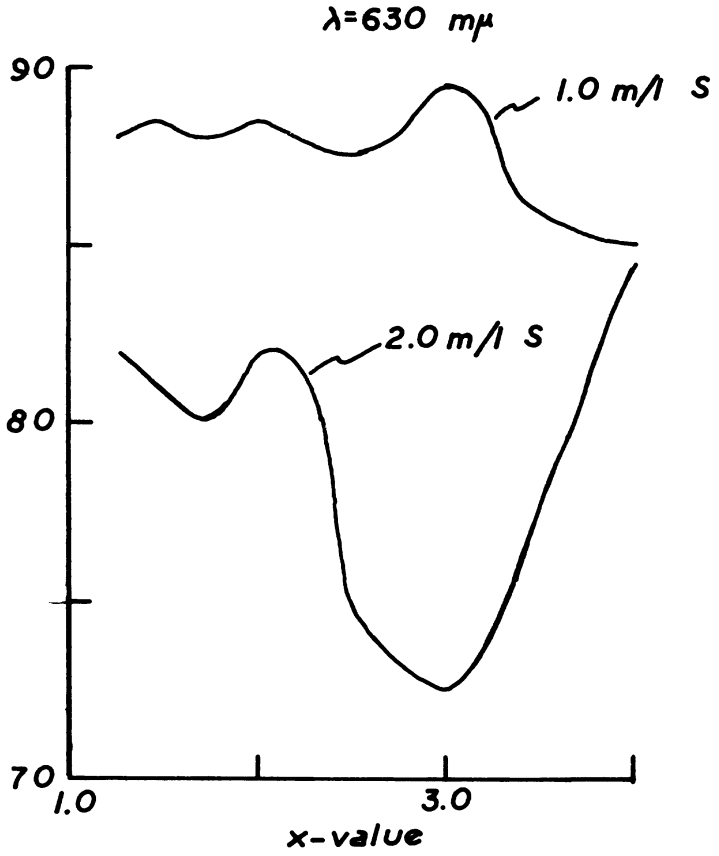

Figure 7. Calibration curves for the spectrophotometric determination of polysulfide sulfur.

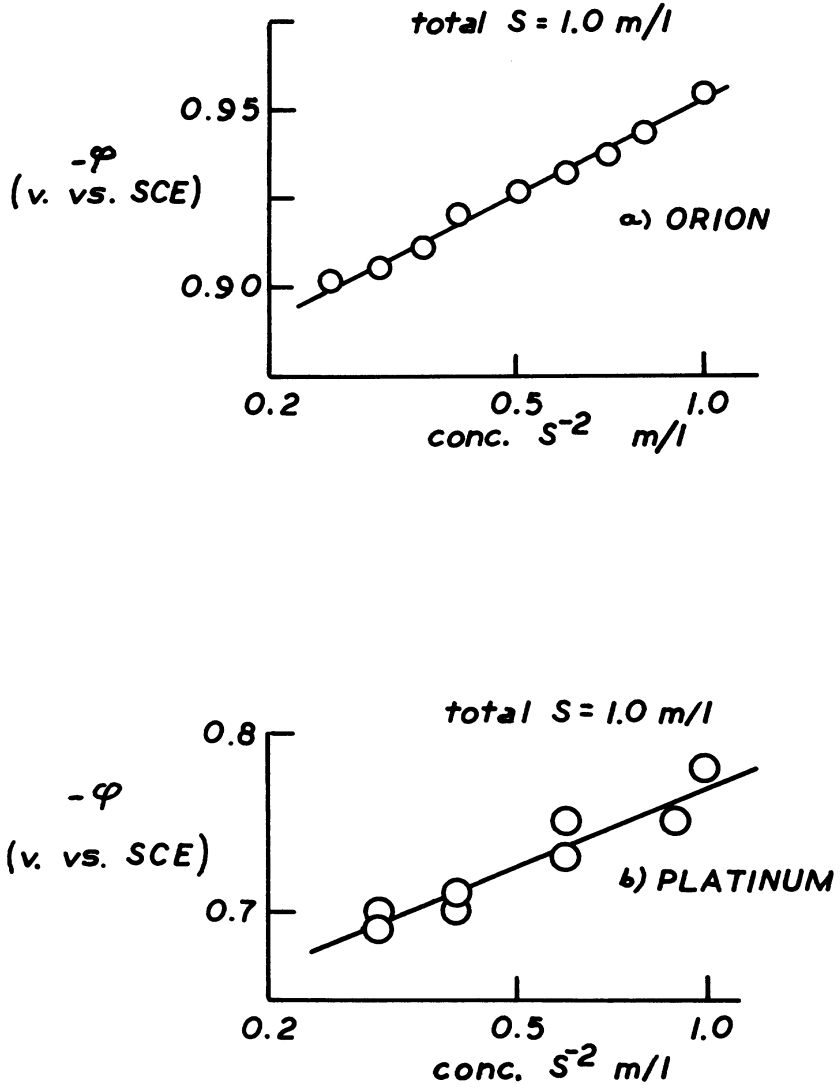

Figure 8. Calibration curves for polysulfide sulfur using electrode potential measurements at (a) Orion specific ion electrode and (b) a platinum electrode.

7. ANODIC BEHAVIOR OF SULFIDE ION ELECTRODES

The anodic behavior of the sulfide-polysulfide redox couple was studied on smooth platinum and carbon electrodes. The overall reaction is

$$x\, S^{-2} \rightarrow S_x^{-2} + (2X-2)e^- \qquad (7\text{-}1)$$

The mechanism of the reaction is unknown, but the following steps among others are possible:

$$S^{-2} \rightarrow S_{ads}^{-1} + e^- \qquad (7\text{-}2)$$

$$S_{ads}^{-1} \rightarrow S_{ads} + e^- \qquad (7\text{-}3)$$

$$S_{ads} + S^{-2} \rightarrow S_2^{-2} \qquad (7\text{-}4)$$

$$S^{-2} + S_x^{-2} \rightarrow S_{x+1}^{-3} + e^- \qquad (7\text{-}5)$$

$$S_{x+1}^{-3} \rightarrow S_{x+1}^{-2} + e^- \qquad (7\text{-}6)$$

While the mechanism was not pertinent to the analysis at hand, the complexity of the kinetics derived from the polarization curves indicated that a simple kinetic model was not feasible.

A. DETERMINATION OF REACTION ORDERS

The rate of reaction of an electrochemical oxidation may be written

$$i_p = k\,[\mathrm{Red}]^{\gamma} \qquad (7\text{-}7)$$

where k is a rate constant (see equation (3-11), [Red] represents the reduced form of the chemical species (here, S^{-2}) and γ is the reaction order with respect to the reduced form of the species. The following relation is true if

the reaction mechanism is not excessively complex

$$\left(\frac{\partial \log i_p}{\partial \log [\text{Red}]}\right)_{\varphi_{i,T}} = \gamma \qquad (7\text{-}8)$$

Equation (7-8) shows that log-log plots of current density-concentration of the reduced form of the species (at fixed potential and temperature) should yield a straight with slope γ. This situation is normally encountered. Figure 9 effectively supports this prediction over a limited concentration range. The data in Figure 9 were obtained on smooth platinum electrodes at 35°C with a total sulfur concentration of 1.0 g moles/liter. Empirically, Figure 9 shows that the reaction order with respect to sulfide ion is one for concentrations below 0.7 g moles/liter.

More extensive reaction order determinations were performed using carbon electrodes (Stackpole 139). Equation (7-8) was used as the basis for the determination of the reaction order. The data are shown in Figure 10a. It is evident that at the lower temperatures, viz., 35 and 40°C, equation (7-8) is obeyed and the slope is 1.0 for concentrations below 0.7 g moles/liter. However, at the higher temperatures, the simple approach to reaction order determination is invalid. Although there is no physical basis for the plot, Figure 10b is presented to show that, when the "normal" electrochemical approach to reaction order gives "meaningless" data, an apparent reaction order of 0.5 with respect to sulfide ion is observed. From these observations it is evident that the rate expression involves both sulfide ion and dissolved sulfur and that the reaction orders of these species could vary with temperature.

The reader may argue that the approach used here to determine the reaction order with respect to sulfide ion and dissolved sulfur is intuitively incorrect and, consequently, prejudices the validity of the overall study. This is not the case. In most studies of electrochemical kinetics the approach used here would have provided a linear plot with a "rational" value of reaction order. Viewing the carbon electrode studies ex post facto, it would have been better to have determined the reaction order with respect to sulfide ion at fixed concentration of dissolved sulfur. However, in the face of other data (see below), there is no assurance that straight lines of constant slope would emerge from the data.

A case in point is the determination of the effect of alkali on the rate of the reaction. Figure 11 shows a log-log plot of the current density-concentration of hydroxyl ion (at fixed sulfide-sulfur concentrations). At low temperatures (35 and 40°C, the latter is not shown) a concave downward curve is observed. At 45°C the slope of the line is 0.2 while the higher temperatures (50 and 60°C) give slopes of 0.5. Consequently, even the results of the

"normal chemical" approach to reaction order determination suggest that the kinetic picture is extremely complex.

If interest in the sulfide-sulfur reaction continues, it will be imperative to restudy the kinetics in greater detail. However, it appears that a single rate expression of "standard" form which includes all combinations of concentrations and temperatures is unlikely. An empirical rate expression cannot be derived from the data obtained; however, such an expression is feasible if sufficient data are available for a regression analysis.

B. ACTIVATION ENERGY

The activation energy for the oxidation of sulfide ions can be determined from

$$\left(\frac{\partial \log i_p}{\partial (1/T)}\right)_{\varphi_{i,C}} = -\frac{E^{\ddagger}}{2.3R} \qquad (7\text{-}9)$$

i.e., the variation of the log of the current density with reciprocal temperature at constant electrode potential and concentrations of all species is proportional to the activation energy. Figure 12 shows plots used to obtain the activation energy for the oxidation reaction. Table I lists the activation energies obtained for solutions containing less than 0.7 g moles/liter of S^{-2}.

TABLE I

EXPERIMENTAL VALUES OF ACTIVATION ENERGY FOR THE OXIDATION OF SULFIDE ION
(φ_i = -0.7 v vs. S.C.E.; Stackpole 139; Total S = 1.0 g mole/liter)

$[S^{-2}]$	$[OH^-]$	$E^{\ddagger}$ (kcal/g mole)
0.2	1.0	9
0.4	1.0	12
0.6	0.5	10
0.6	1.0	8
0.6	2.0	15

On the basis of the absence of a trend with respect to sulfide ion or caustic it may be assumed that the activation energy is constant, viz., 11 ± 2 kcal/g mole. The magnitude of the activation energy is (a) higher than that for convective mass transport, and (b) on the low side for chemical or electrochemical reactions. These observations indicate that, unless the feed stream is hot, it is problematic whether heating the feed would serve to increase the rate of reaction (or, for an electrolysis cell, decrease the terminal voltage) significantly.

C. STANDARD SPECIFIC RATE CONSTANT

A precondition for the determination of the standard specific rate constant is some knowledge of the reaction orders of the reacting species. It is evident that, the analysis given in the Progress Report last summer notwithstanding, it is not feasible to determine the value of the standard specific rate constant on the basis of the number of experiments given here. With further experimentation the standard specific rate constant could be obtained by the regression analysis mentioned above.

D. POLARIZATION BEHAVIOR

The anodic polarization curves for the oxidation of sulfide ion at platinum and carbon electrodes are presented in Figures 13 and 14. The conditions associated with the various curves are given on the respective drawings. For Figure 14, the filled symbols represent extrapolations of the φ-t curves to zero time (this is an approximation of the data which corrects for unsteady-state behavior and was feasible through the use of a storage oscilloscope for the φ-t transients). The data with the carbon electrode are generally an order of magnitude better than the platinum experiments, i.e., at a given potential the current densities differed by a factor of ten. Since the real area of the carbon electrode is greater than ten times that of the smooth platinum, the "true" catalytic properties of platinum are better than those of the carbon electrodes.

E. FURTHER COMMENTS ON COMPLEX KINETICS

In the foregoing, allusion was made to "complex kinetics." In order to clarify what is meant by this term, the following hypothetical rate expression will be considered

$$r = \frac{k_1[S^{-2}][S][OH^-] + k_2[S^{-2}]^2[S][OH^-]}{K_3[S][OH^-] + k_4[S]^{1/2}[OH^-]^{1/2}} \qquad (7\text{-}10)$$

For ease in discussing the phenomena, the following simplifications are made

$$r = \frac{A + B}{C + D} \tag{7-11}$$

At low temperatures: $A > B$ and $C > D$; then the rate becomes

$$r = \frac{k_1 [S^{-2}]}{k_3} \tag{7-12}$$

which predicts first order kinetics for S^{-2} with a specific rate constant equal to k_1/k_3. At temperatures $\geq 50°C$: A = Band C < D; then the rate becomes

$$r = \frac{[S^{-2}] [S]^{1/2} [OH^-]^{1/2} (k_1 + k_2[S^{-2}])}{k_4}$$

which predicts half-order kinetics for S and OH^-, indeterminate order for S^{-2} and an "unspecified" rate constant. For intermediate temperatures: A = B and C = D. The orders and rate constant are indeterminate under these conditions.

Rate expressions similar to equation (7-10) have been observed for a number of chemical reactions. However, they are developed only after a complete mechanistic analysis. The system at hand probably obeys a similar rate low, but, in the absence of a complete mechanistic analysis, the authors must allude to a "complex kinetic" expression.

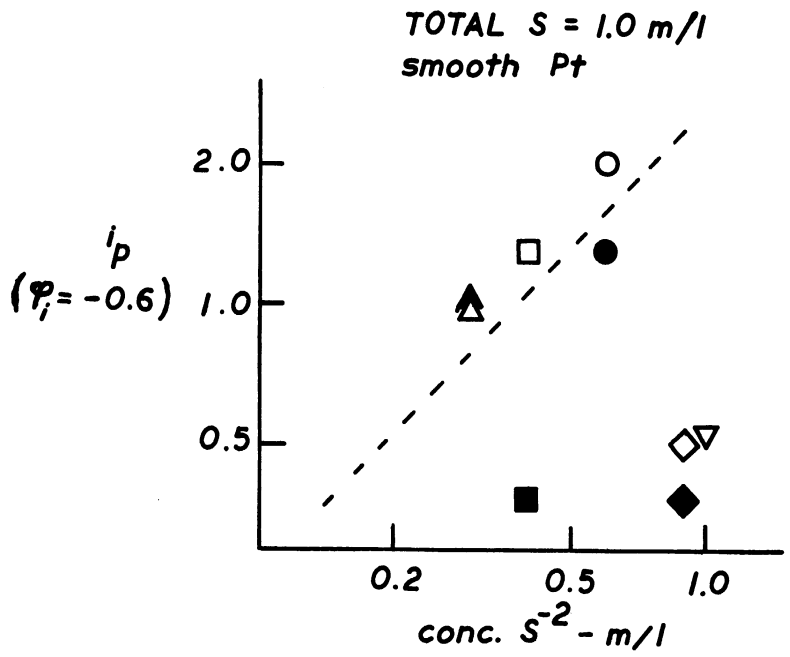

Figure 9. Determination of the reaction order data for the oxidation of sulfide ion on platinum.

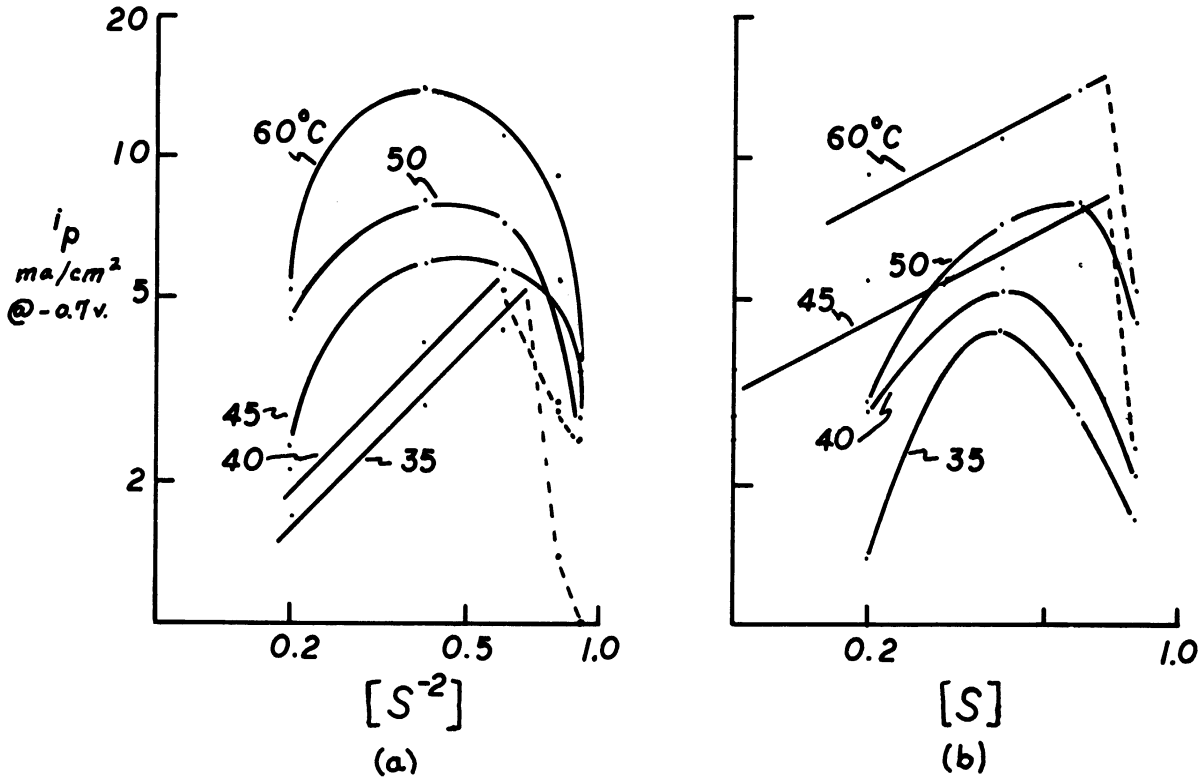

Figure 10. Determination of the reaction order for the oxidation of sulfide ion on carbon electrodes.

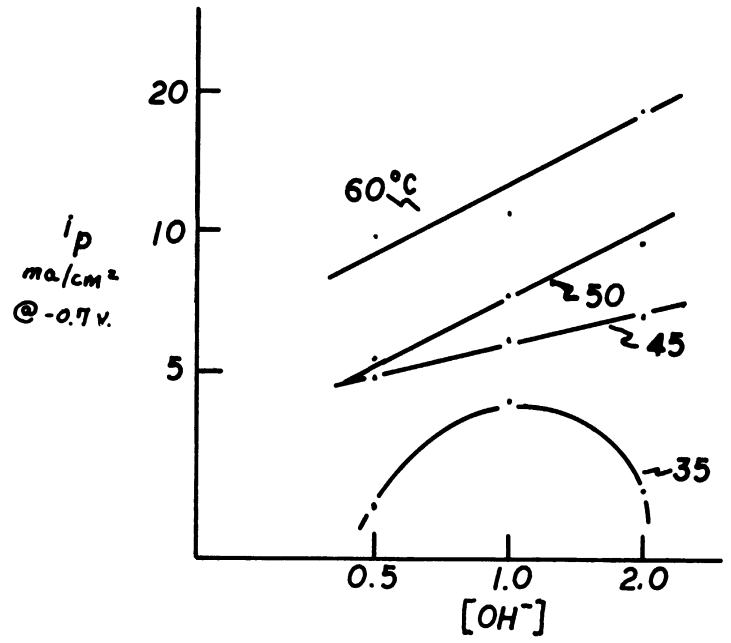

Figure 11. Determination of the reaction order with respect to hydroxyl ion for the oxidation of sulfide ion on carbon electrodes.

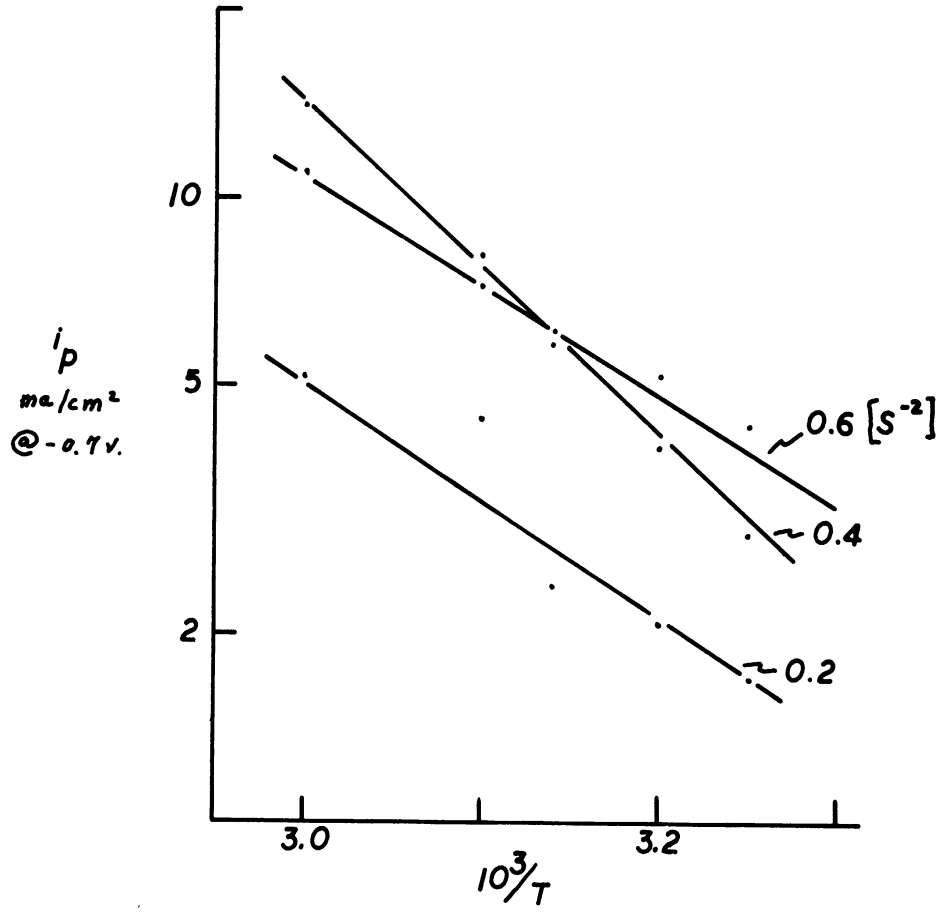

Figure 12. Determination of the activation energy for the oxidation of sulfide ion on carbon electrodes.

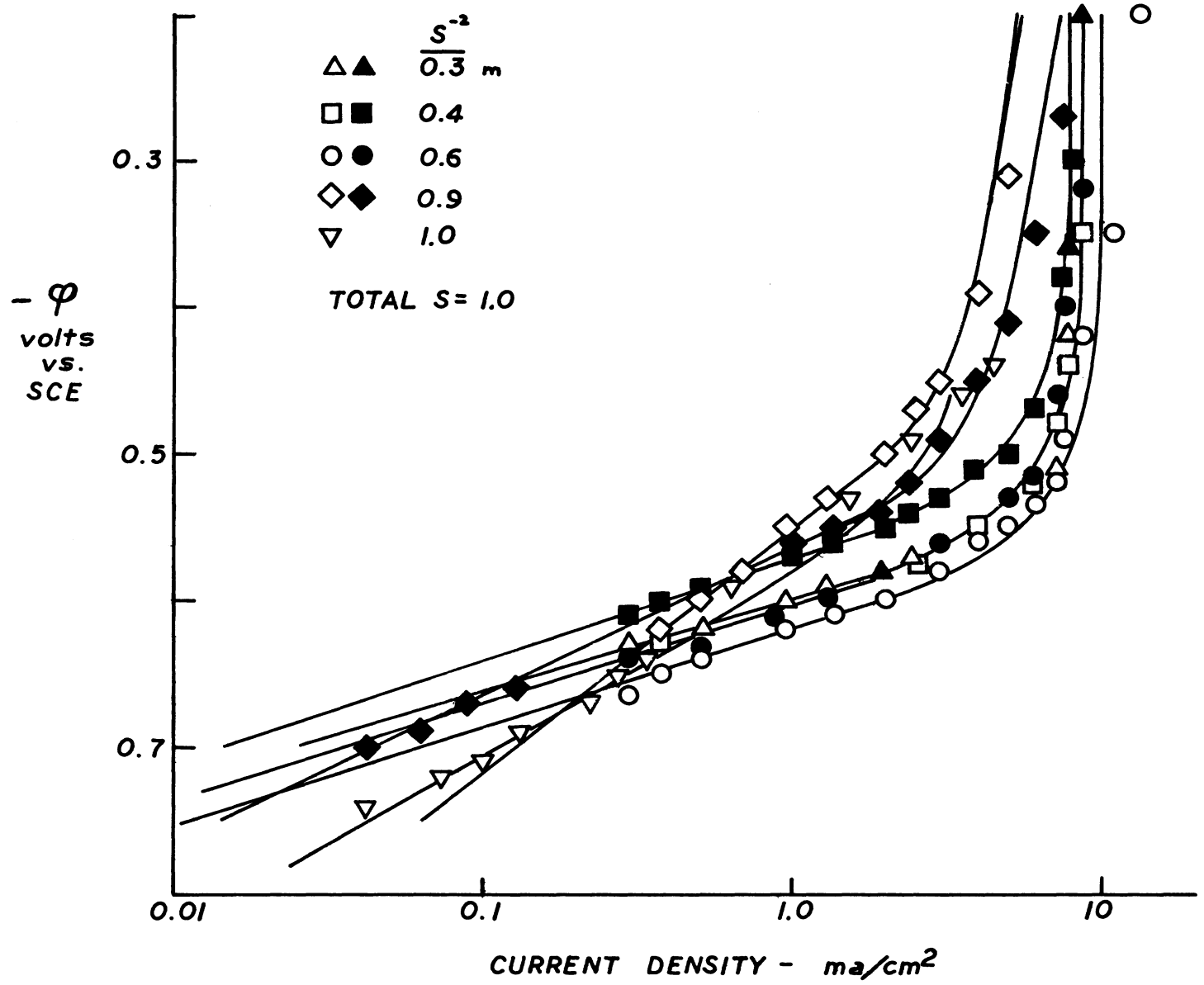

Figure 13. Polarization behavior of platinum electrodes for the oxidation of sulfide ion.

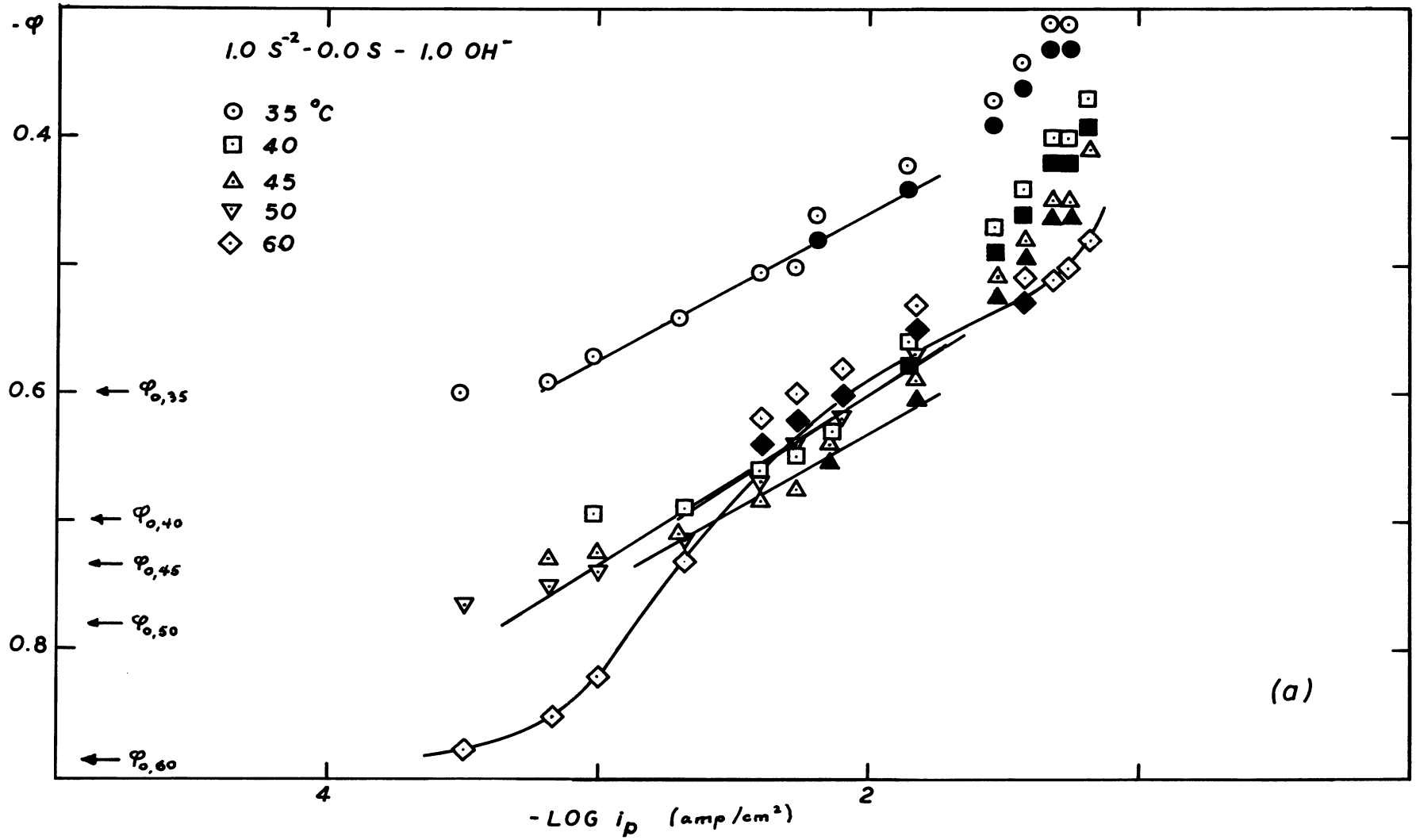

Figure 14. Polarization behavior of carbon electrodes for the oxidation of sulfide ion.

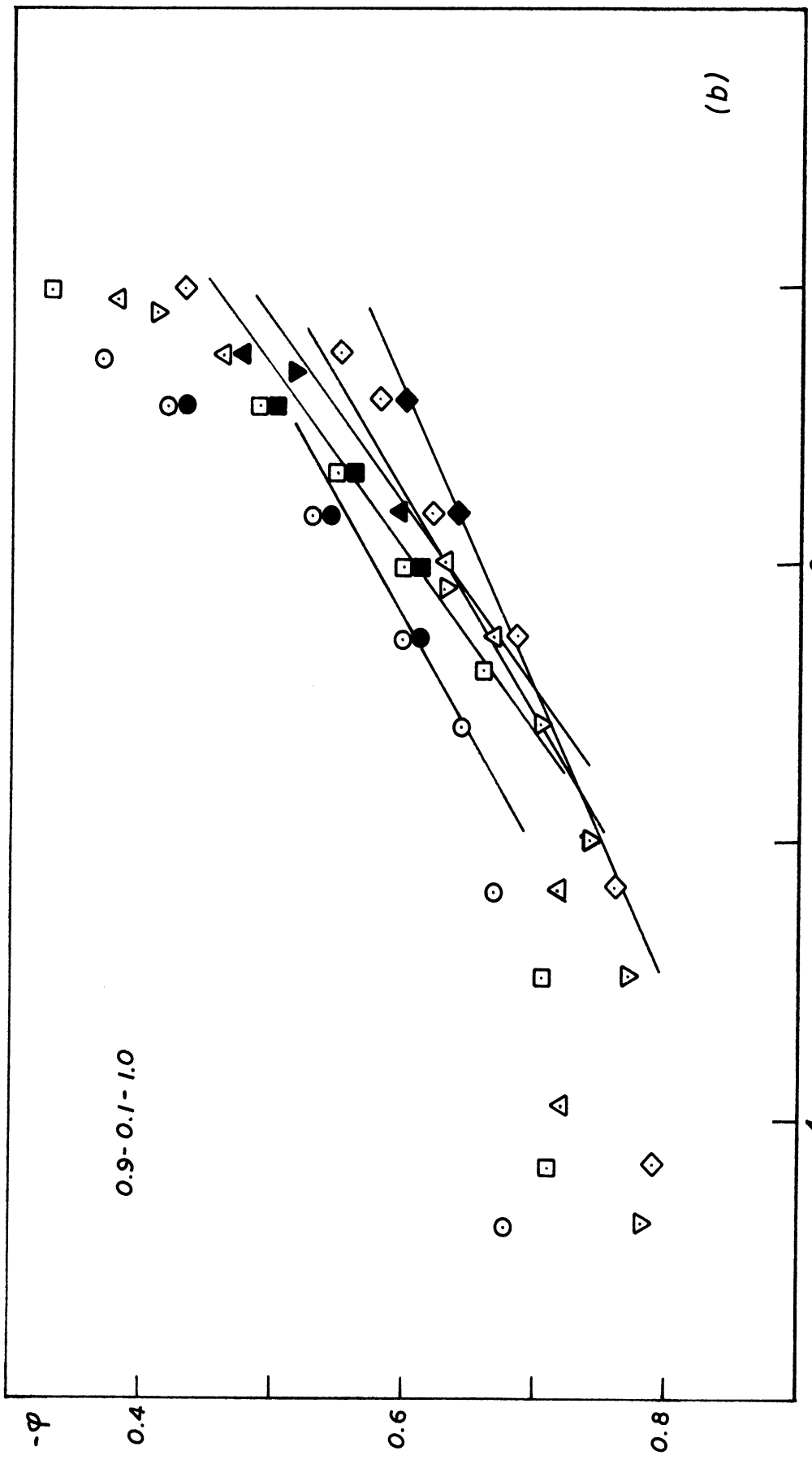

Figure 14. (Continued)

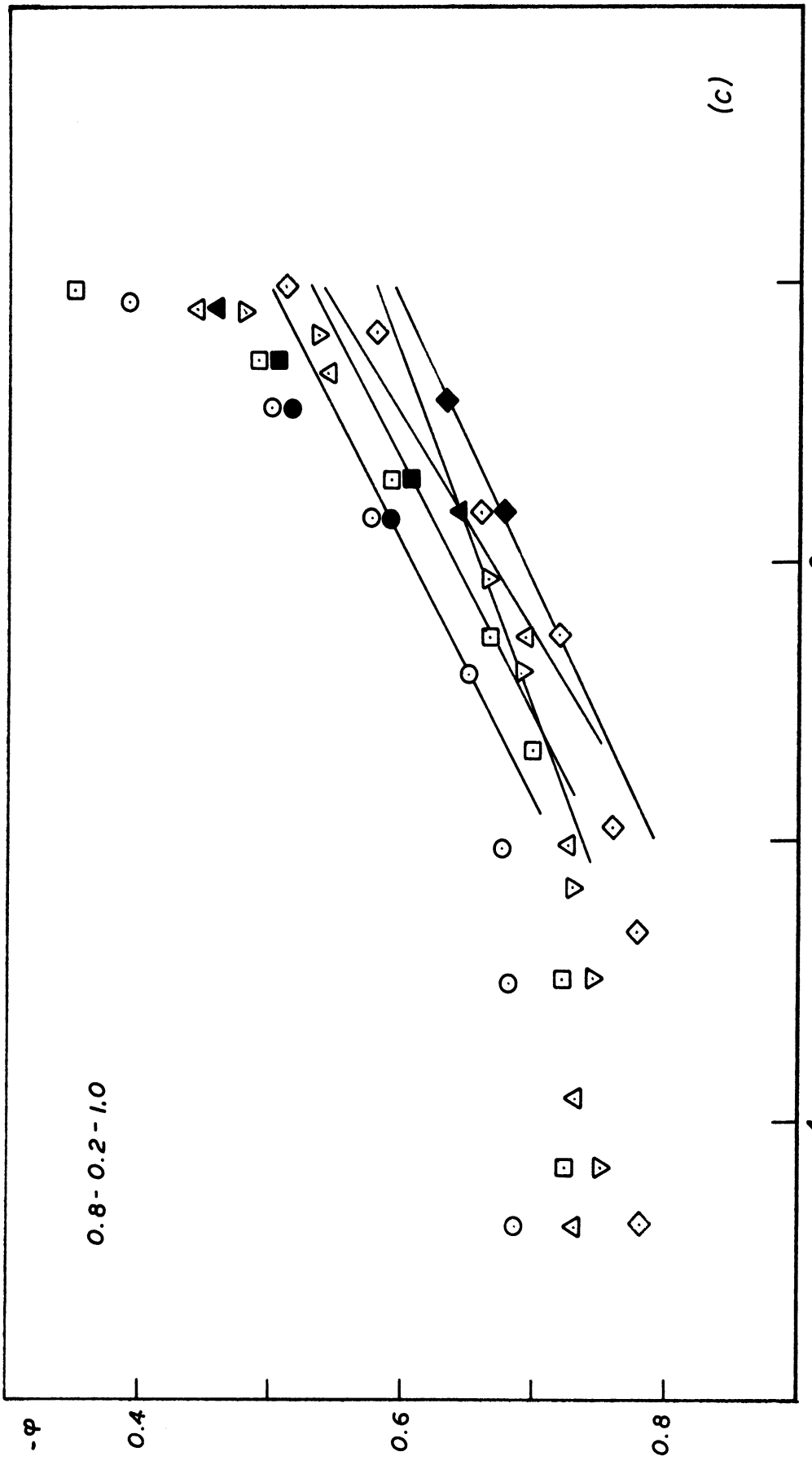

Figure 14. (Continued)

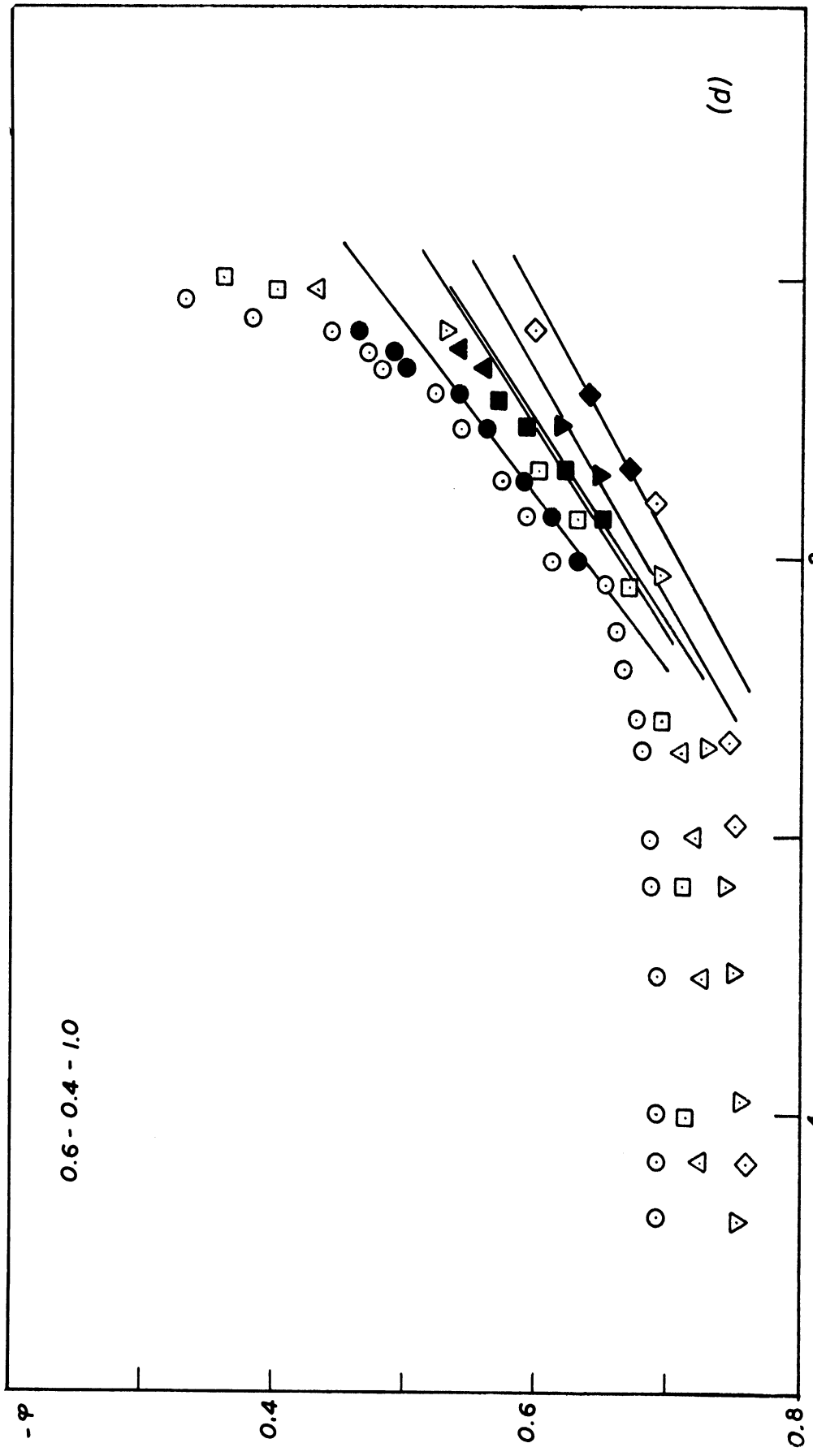

Figure 14. (Continued)

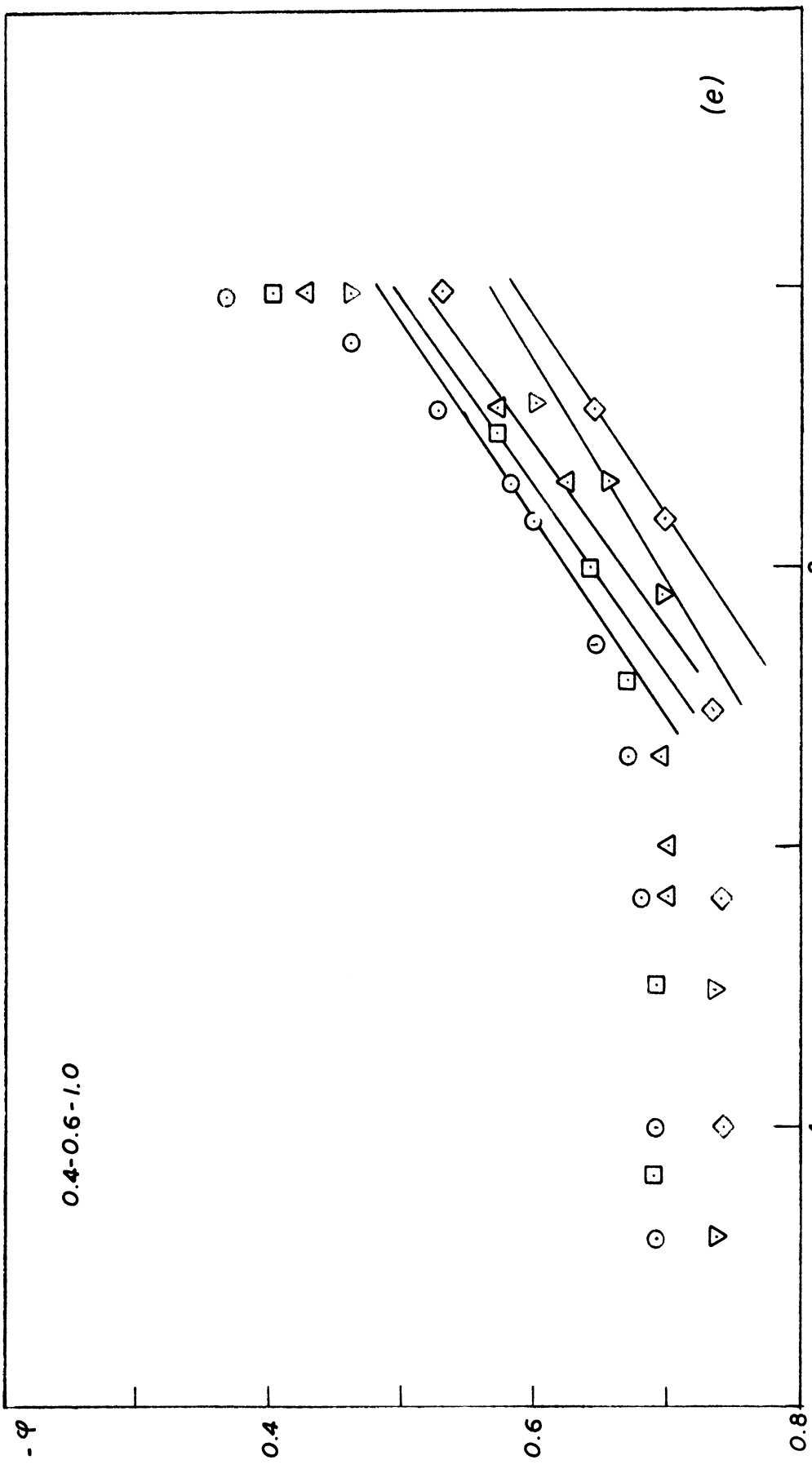

Figure 14. (Continued)

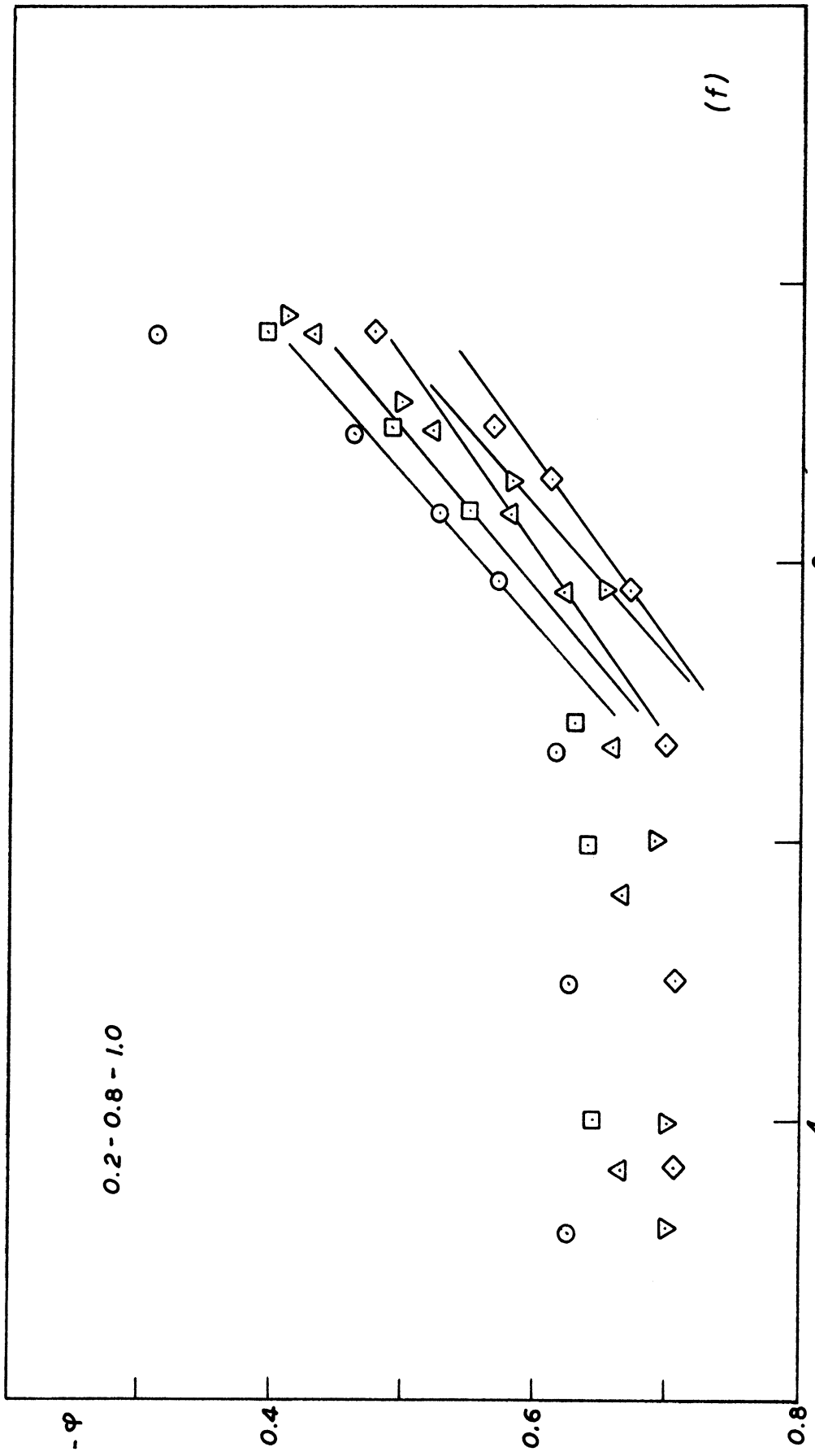

Figure 14. (Continued)

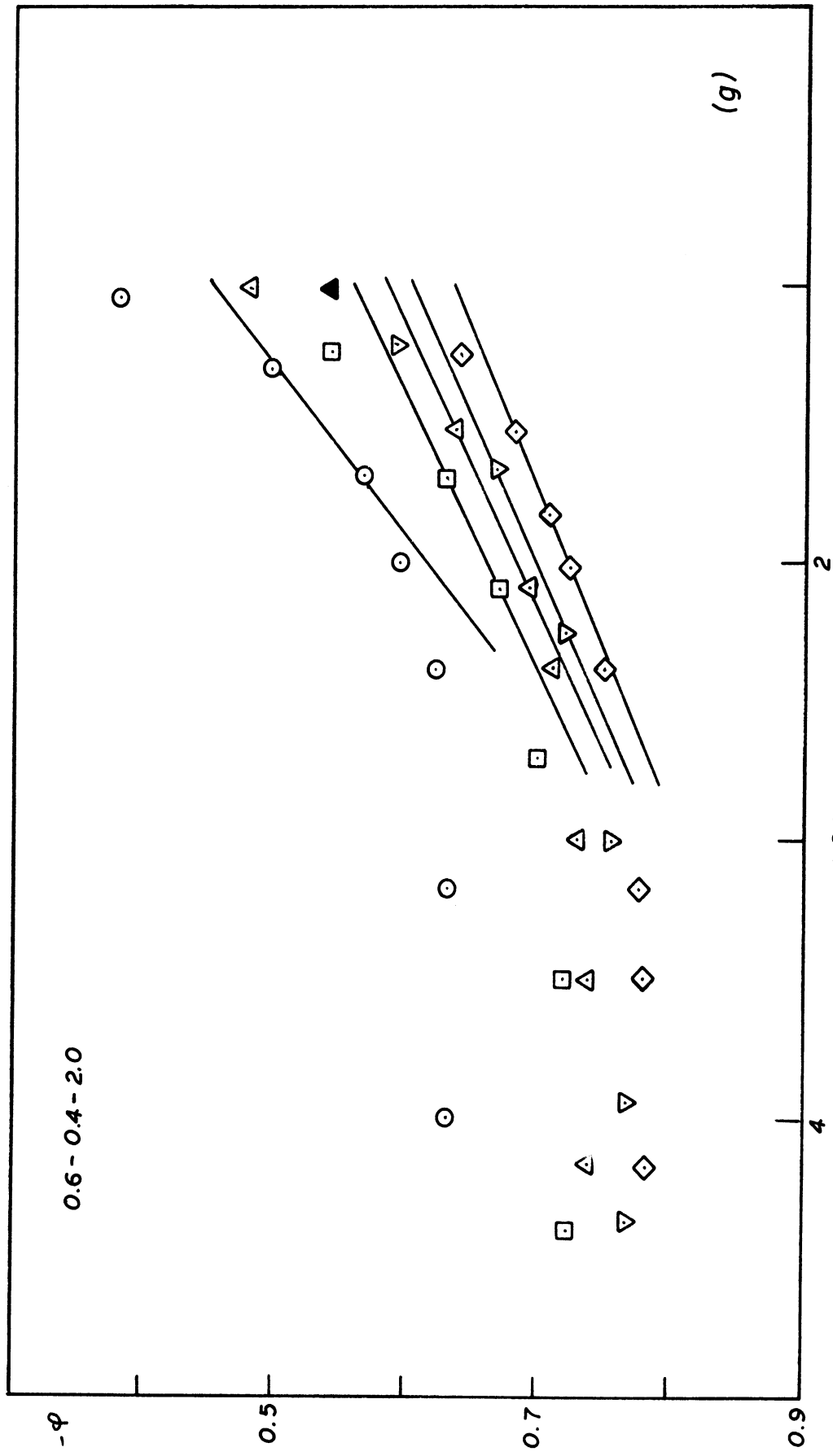

Figure 14. (Continued)

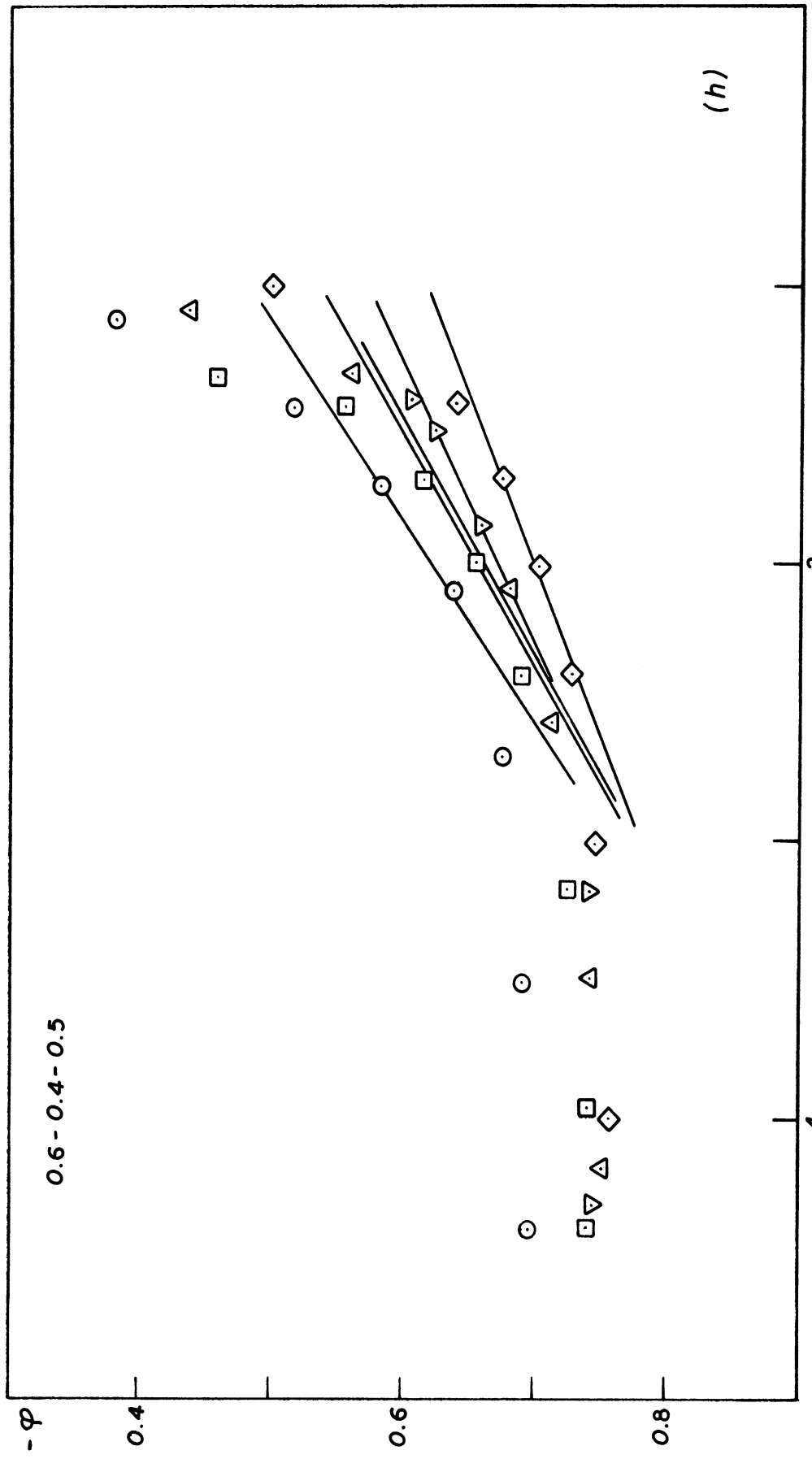

Figure 14. (Concluded)

8. ANODIC AND CATHODIC BEHAVIOR OF OXYGEN ELECTRODES

Preliminary experiments on the anodic and cathodic behavior of Union Carbide T2 and T3 electrodes using air as the oxygen source were carried out in 5M NaOH at 35°C. The results indicate that neither electrode is reversible to the oxygen-water system, i.e., the observed open circuit voltage more closely approximates the peroxide-oxygen system (this phenomenon has been observed by Kordesch and others with carbon electrodes). However, the T3 electrode (nickel side toward the electrolyte) was found to be extremely unstable as evidenced by the wide spread between the anodic and cathodic polarization curves (see Figure 15). Further, it was noted that the polarization characteristics deteriorated with subsequent polarizations.

On the other hand, the T2 electrode (carbon contacting the electrolyte), albeit not reversible to the oxygen-water system, gave better cathodic polarization characteristics at all current densities and better anodic properties at high current densities. In comparing the cathodic properties of the T3 it is evident that this electrode could be used in a "fuel cell" and/or mixed potential configuration for polysulfide production without the use of an external DC power source.

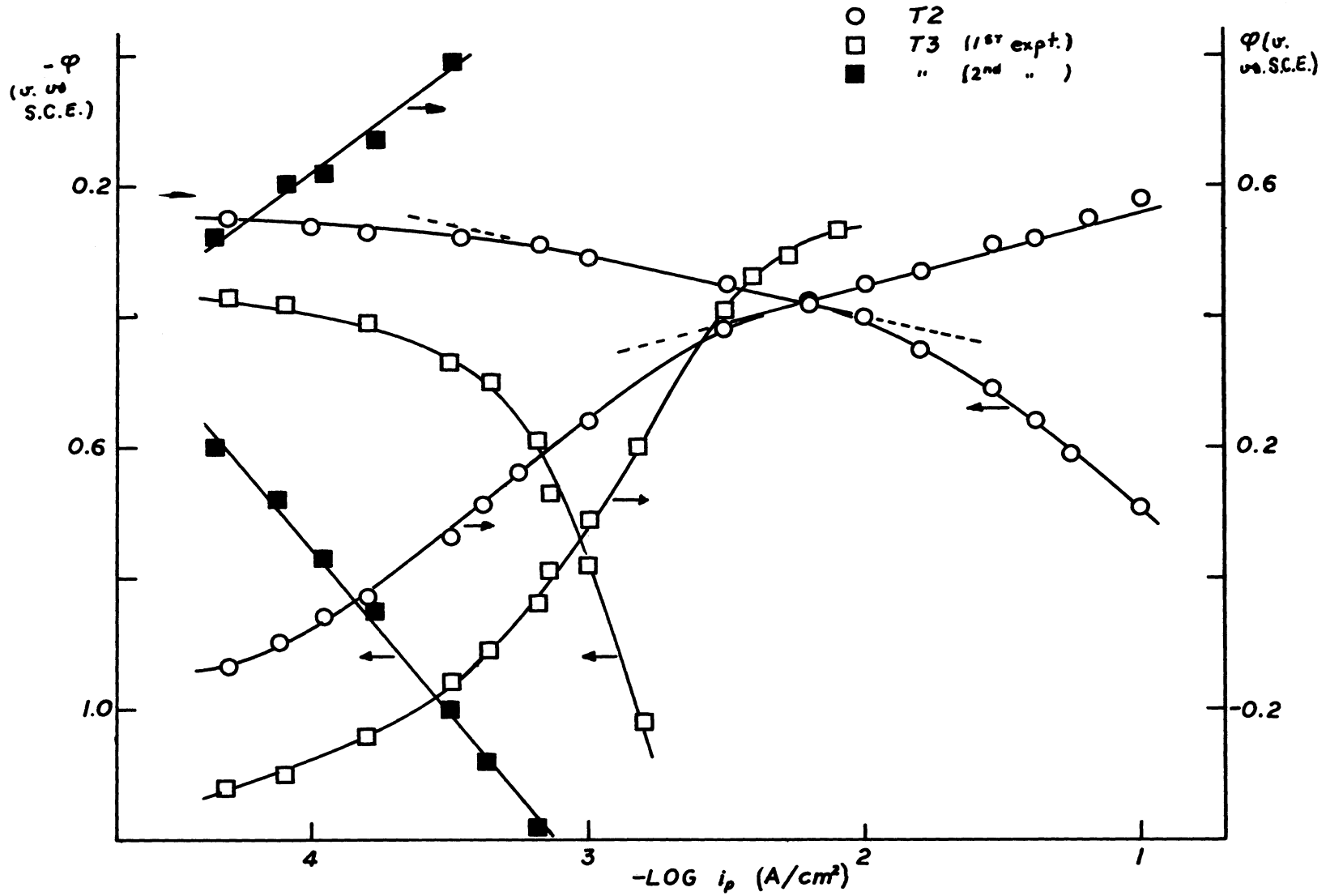

Figure 15. Anodic and cathodic polarization behavior of Union Carbide electrodes for the air-alkali system at 35°C.

9. HYDROGEN EVOLUTION ON CARBON STEEL ELECTRODES

In conventional electrolysis cells the cathodic half cell reaction does not permit the overall cell reaction to be operated in the fuel cell or mixed potential mode. The hydrogen evolution reaction is a reaction typical of this type of cathode. In order to complete the analysis, preliminary experiments of hydrogen evolution (with the generation of caustic) on carbon steel electrodes were attempted. Quantitative data are not reported for this system since no steady-state data were obtained. It is evident from the data which were obtained that: (a) the carbon steel was covered with an oxide film which was slowly reduced during the hydrogen evolution reaction (this caused the cathodic overvoltage to increase slowly, but perceptibly, during the electrolysis), and (b) an electrolysis cell generating polysulfide and hydrogen (with caustic) would operate at terminal voltages in excess of 0.7 volt (excluding internal resistance drop) at a current density of 10 ma/cm^2.

10. CONCLUSIONS AND RECOMMENDATIONS

The conclusions and recommendations to be made by the authors are colored both by the report itself and the senior author's personal knowledge of Mead's particular immediate interests. It will be meaningful to review the steps leading to the proposal, the underlying premises of the proposal and the subsequent changes in emphasis at Mead leading to the termination of the research contract.

In the fall of 1968 it became evident to Mead and the senior author that the Mead Research Laboratories were effectively unable to attempt an in-depth study of electrolysis cells and fuel cell-type electrochemical reactors. The senior author's laboratory seemed to be the facility most likely to fill this requirement. For this reason a research proposal was presented to Mead in December, 1968 and, subsequently, accepted by Mead. The emphasis for the research was placed in three broad categories: theory, single redox reaction polarization studies, and reactor prototype systems. Although it was proposed that results could be forthcoming from all categories, a complete analysis was obtained only in the theoretical area. Moderate success was obtained in the polarization studies (unfortunately, the primary emphasis involved a system which, although of significance to Mead prior to the fall of 1969, is of subsidiary interest at present). The prototype reactor is at present only a "plumbing" success (however, electrolysis cells are currently of no interest to the sponsor).

In the opinion of the senior author, the underlying premises of the proposal were: (a) development of a theoretical basis for the analysis of electrochemical reactors, and (b) demonstration of a research philosophy whereby meaningful data may be obtained on practical chemical systems which might exploit the theoretical treatment. In this regard, the senior author respectfully submits that the research reported herein is a success. Consider for the moment the change in research philosophy at Mead during the calendar year of 1969. The thrust for commercialization has passed from electrolytically or "fuel cell" generated polysulfide to mixed potential electrolysis generation to an exploitation of mixed potential systems in general. While this has caused drastic changes in the approach to the problem at Mead, it has had virtually no effect on the research project at Michigan. This was not due to an oblivious attitude toward the plight of the sponsor. It derives from the fundamental understanding that all of the pehnomena under discussion obey the same basic laws of electrochemistry.

Consider the data from this report which are shown in Figure 16. The open circles represent the cathodic polarization (oxygen reduction) of a Union Carbide T2 electrode operating on air at 35°C and atmospheric pressure (see Figure 15); the solid circles represent the oxidation of sulfide ions

(0.8M S^{-2}, 0.2M S and 1M OH^{-}) at a Stackpole 139 carbon anode at 35°C (see Figure 14c). The intersection of these two curves is at the point where these two half-cell reactions would undergo mixed potential electrolysis (MPE). To the left of this point describes the fuel cell mode of a cell with the conditions listed above. To the right of the MPE point is the region which describes the driven fuel cell mode of this system. Thus, two polarization curves in conjunction with the theoretical aspects of this report may be used to describe three physically (and economically) different operational dispositions of the system. If an appropriate number of anodic and cathodic polarization curves are obtained, similar comparisons are feasible.

It is concluded and recommended that single redox reaction polarization studies represent the most logical approach to the studies of mixed potential electrolysis systems. It is further recommended that, in the light of the complex nature of the electrode reactions presented in this report, this effort be supplemented by extramural research and consulting by competent personnel. The totality of this study (as in the fall of 1968) falls outside the competence of the majority of the Mead Research personnel currently associated with the project.

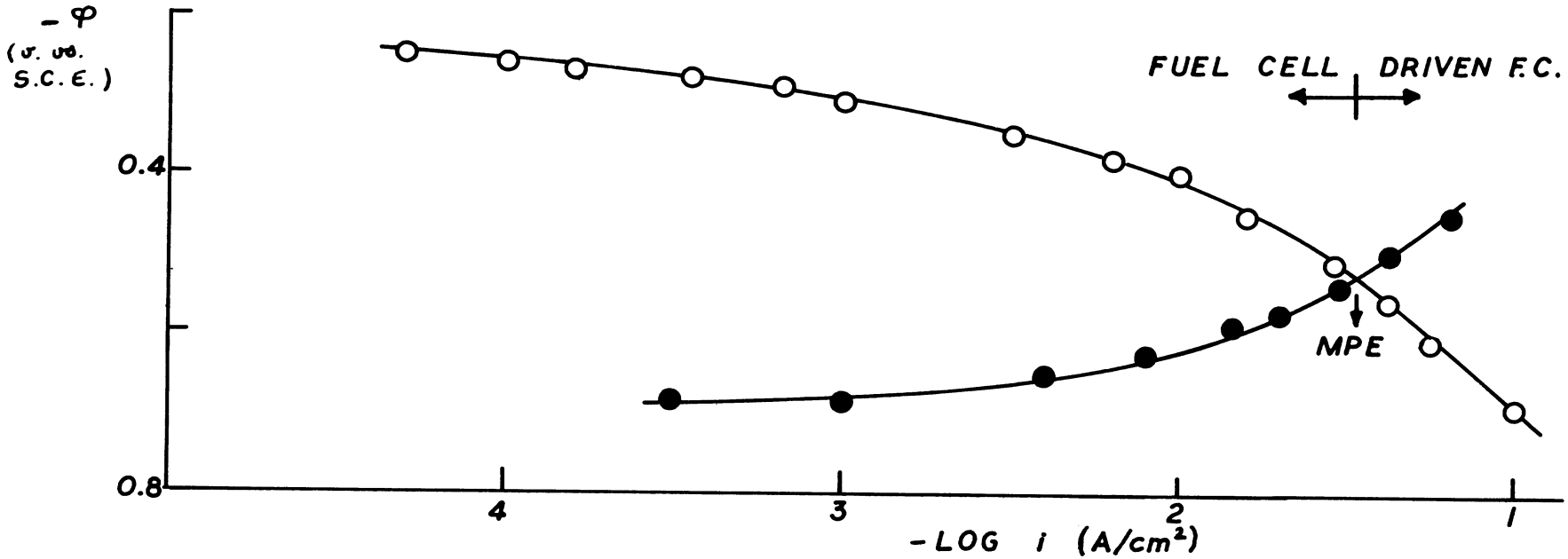

Figure 16. Demonstration of the utility of "fundamental" half-cell studies to the phenomena of fuel cell, driven fuel cell, and mixed potential electrolysis systems.

11. REFERENCES

1. O. Levenspiel. Chemical Reaction Engineering. Wiley, New York, 1962.

2. F. M. Donahue. Fundamentals of Electrochemical Engineering. Engineering Summer Conferences, The University of Michigan, Ann Arbor, 1969.

3. G. C. Smith. Private Communication, 1969.

4. F. M. Donahue. Discussion at the Central Research Laboratories, Mead Corporation, 1969.